Research paper

Modelling the hydrodynamic response of a floating offshore wind turbine – a comparative study

Shimin Yu [a], Edward Ransley [b], Ling Qian [a,*] , Yang Zhou [a], Scott Brown [b], Deborah Greaves [b], Martyn Hann [b], Anna Holcombe [b], Emma Edwards [b], Tom Tosdevin [b], Sudhir Jagdale [w], Qian Li [c], Yi Zhang [c], Ningbo Zhang [c], Shiqiang Yan [c], Qingwei Ma [c], Bonaventura Tagliafierro [d,h], Salvatore Capasso [e], Iván Martínez-Estévez [f], Malin Göteman [g], Hans Bernhoff [g], Madjid Karimirad [h], José M. Domínguez [f], Corrado Altomare [d], Giacomo Viccione [e], Alejandro J.C. Crespo [f], Moncho Goméz-Gesteira [f], Claes Eskilsson [i], Gael Verao Fernandez [j], Jacob Andersen [j], Johannes Palm [k], Francesco Niosi [l], Oronzo Dell'Edera [l], Massimo Sirigu [l], Alberto Ghigo [l], Giovanni Bracco [l], Fuyin Cui [m], Shuling Chen [m], Wei Wang [m], Yueyue Zhuo [m], Yang Li [m], Christophe Peyrard [n,q], William Benguigui [o,p], Matthieu Barcet [o], Fabien Robaux [n,q], Michel Benoit [n,q], Maria Teles [n], Dimitris Ntouras [r], Dimitris Manolas [s,t], George Papadakis [r], Vasilis Riziotis [t], Zhiping Zheng [u], Weicheng Lei [u], Ruizhi Wang [u], Jikang Chen [u], Yanlin Shao [v], Jens Visbech [x], Harry B. Bingham [v], Allan P. Engsig-Karup [x], Yiming Zhou [y], Yefeng Cai [y], Haisheng Zhao [y], Wei Shi [y], Xin Li [y], Xinmeng Zeng [z], Yingjie Xue [aa], Tiegang Zhuang [ab], Decheng Wan [aa], Gaspard Engel [ac], Matthieu Tierno [ac], Guillaume Ducrozet [ac], Benjamin Bouscasse [ac], Vincent Leroy [ac], Pierre Ferrant [ac], Gabriel Barajas [ad], Javier L. Lara [ad]

[a] *Manchester Metropolitan University, UK*
[b] *University of Plymouth, UK*
[c] *City, University of London, UK*
[d] *Laboratori d'Enginyeria Marítima, Universitat Politècnica de Catalunya - BarcelonaTech (UPC) Barcelona, Spain*
[e] *Department of Civil Engineering, University of Salerno, Italy*
[f] *Environmental Physics Laboratory, CIM-UVIGO, Universidade de Vigo, Spain*
[g] *Dept. of Electrical Engineering, Uppsala University, Sweden*
[h] *School of Natural and Built Environment, Queen's University Belfast, UK*
[i] *RISE - Research Institutes of Sweden*
[j] *Aalborg University*
[k] *Sigma Energy & Marine AB, Sweden*
[l] *Department of Mechanical and Aerospace Engineering (DIMEAS), Politecnico di Torino, Turin, Italy*
[m] *Jiangsu University of Science and Technology, China*
[n] *EDF R&D, Laboratoire National d'Hydraulique et Environnement (LNHE), Chatou, France*
[o] *EDF R&D, Dept. Mécanique des Fluides, Energies et Environnement (MFEE), Chatou, France*
[p] *IMSIA, UMR 9219 EDF/CNRS/CEA/ENSTA ParisTech, Palaiseau, France*
[q] *Saint-Venant Hydraulics Laboratory (EDF R&D, ENPC), Chatou, France*
[r] *School of Naval Architecture & Marine Engineering, National Technical University of Athens*
[s] *iWind Renewables PC*
[t] *School of Mechanical Engineering, National Technical University of Athens*
[u] *College of Shipbuilding Engineering, Harbin Engineering University, Harbin, 150001, China*
[v] *Department of Civil and Mechanical Engineering, Technical University of Denmark, Denmark*
[w] *Independent Engineering Consultant, London, UK*
[x] *Technical University of Denmark, Department of Applied Mathematics and Computer Science, Denmark*
[y] *Dalian University of Technology, College of Engineering, China*
[z] *Ocean University of China, Qingdao, China*

* Corresponding author.
E-mail address: l.qian@mmu.ac.uk (L. Qian).

[aa] *Computational Marine Hydrodynamic Lab (CMHL), School of Naval Architecture, Ocean and Civil Engineering, Shanghai Jiao Tong University, Shanghai, China*
[ab] *Key Laboratory of Far-shore Wind Power Technology of Zhejiang Province, Huadong Engineering Corporation Limited, Hangzhou, China*
[ac] *Nantes Université, École Centrale Nantes, CNRS, LHEEA, Nantes, France*
[ad] *IHCantabria - Instituto de Hidráulica Ambiental de La Universidad de Cantabria, Santander, Spain*

ARTICLE INFO

ABSTRACT

This paper summarises the work conducted within the 1st FOWT (Floating Offshore Wind Turbine) Comparative Study organised by the EPSRC (UK) 'Extreme loading on FOWTs under complex environmental conditions' and 'Collaborative computational project on wave structure interaction (CCP-WSI)' projects. The hydrodynamic response of a FOWT support structure is simulated with a range of numerical models based on potential theory, Morison equation, Navier-Stokes solvers and hybrid methods coupling different flow solvers. A series of load cases including the static equilibrium tests, free decay tests, operational and extreme focused wave cases are considered for the UMaine VolturnUS-S semi-submersible platform, and the results from 17 contributions are analysed and compared with each other and against the experimental data from a 1:70 scale model test performed in the COAST Laboratory Ocean Basin at the University of Plymouth. It is shown that most numerical models can predict similar results for the heave response, but significant discrepancies exist in the prediction of the surge and pitch responses as well as the mooring line loads. For the extreme focused wave case, while both Navier–Stokes and potential flow base models tend to produce larger errors in terms of the root mean squared error than the operational focused wave case, the Navier-Stokes based models generally perform better. Given the fact that variations in the solutions (sometimes large) also present in the results based the same or similar numerical models, e.g., OpenFOAM, the study highlights uncertainties in setting up a numerical model for complex wave structure interaction simulations such as those involving a FOWT and therefore the importance of proper code validation and verification studies.

1. Introduction

With the exhaustion of conventional fossil energy and the deterioration of the global climate, exploiting green and renewable energy resources has become a common consensus around the world. Offshore wind, as one of the major renewable resources (Council–GWEC 2023), is expected to play an important role in optimizing the energy structure and mitigating climate change. Most offshore wind turbines installed so far are located in relatively shallow water areas and utilize bottom-fixed support foundations. However, the construction and installation of such foundations in deeper waters (with a depth over 60 meters) are economically not viable due to high costs (Musial, Butterfield et al. 2006, Asim, Islam et al. 2022). To harness the wind energy resources in the deep sea regions with stronger and more stable wind it is necessary to develop floating offshore wind turbine (FOWT) technology (Heronemus 1972; Micallef and Rezaeiha 2021).

In the passing decade a number of FOWT concepts and prototypes have been proposed and developed. As in the design and testing of traditional offshore structures, numerical modelling has become an integral part in evaluating FOWT structures (Chen, Chen et al. 2020; Otter, Murphy et al. 2022) and both potential theory (PT) and computational fluid dynamics (CFD) models have been developed and applied to evaluate the hydrodynamics of FOWTs (Subbulakshmi, Verma et al. 2022). A variety of in-house, open source and commercial codes are available for this purpose – some are specialised computer codes tailored for FOWT applications and some are general fluid dynamics codes. For example, OpenFAST (Fatigue, Aerodynamics, Structures, and Turbulence), is an open-source tool based on the boundary element method (BEM) developed by the National Renewable Energy Laboratory (NREL) (Jonkman and Buhl 2005; Jonkman et al., 2009; Wendt et al., 2015). HAWC2 (the Horizontal Axis Wind turbine simulation Code 2nd generation) is a commercial software developed by the Technical University of Denmark (DTU) (Larsen and Hansen 2007). Orcaflex is also based on the boundary element method for offshore structure analysis developed by Orcina (Orcina 2018). All these tools belong to the family of time-domain analysis, in which wave diffraction and radiation are modelled based on the linear potential flow theory and the viscous effects are accounted for by solving the Morison equation. On the other hand, CFD codes such as STAR-CCM+ and OpenFOAM have also been adopted to model both aerodynamics and hydrodynamics of FOWTs

(Tran and Kim 2015; Dunbar, Craven et al. 2015). Examples of in-house codes include naoe-FOAM-SJTU (Wang et al. 2019), which is developed based on the open-source tool package OpenFOAM, DIEGO – a potential flow solver based on the boundary element method (Peyrard, Benguigui et al. 2023) and QaleFOAM – a hybrid which couples OpenFOAM with a finite element model (Li et al. 2018). As an alternative to mesh-based CFD solvers, particle-based methods such as the Smoothed Particle Hydrodynamics (SPH) method, e.g., DualSPHysics, have also been applied to evaluate hydrodynamic performance of FOWTs (Tan et al. 2023; Tagliafierro et al. 2023; Salis et al. 2024).

To evaluate the applicability and accuracy of various numerical tools and techniques for FOWT applications, comparisons have been made between different solvers in the previous work. For example, the results from the work conducted by Cheng et al. (Cheng, Huang et al. 2019) show that the hydrodynamic damping of a FOWT platform can be better predicted by their code naoe-FOAM-SJTU compared to the codes based on the potential flow theory, i.e., HAWC2 and OpenFAST. Rivera-Arreba et al. (Rivera-Arreba, Bruinsma et al. 2019) applied a fully nonlinear Navier–Stokes (NS) model based on OpenFOAM (version 1606) and a second-order potential-flow solver to evaluate the response of a FOWT floating platform in severe waves, and their results indicate that while the PT based solvers are computationally more efficient they underestimate the amplitude of the heave motion by up to 40% compared to that of the Navier-Stokes model. Wang et al. (Wang, Robertson et al. 2020) performed an uncertainty analysis on CFD simulations of the FOWT platform based on the STAR-CCM+ software in the Offshore Code Comparison, Collaboration, Continued, with Correlation, and uncertainty (OC6) project. It is found that relative to the potential flow model such as OpenFAST, their CFD simulations predicted a higher wave excitation particularly in the surge motion. Li and Bachynski (Li and Bachynski 2021) compared the CFD simulations based on OpenFOAM and the results from an engineering software SIMA (SIMO-RIFLEX) based on the potential flow theory for a FOWT platform under nonlinear wave conditions and found that the CFD solution captures the high-order wave forces more accurately. Lin et al. (Lin, Qian et al. 2021) developed a coupled overset CFD and mooring line model based on OpenFOAM for the analysis of the hydrodynamic responses of FOWTs. Their results indicate that the overset mesh solver can achieve better predictions of the platform motion response compared to the dynamic mesh solver in OpenFOAM.

In recent years, a limited number of code comparative studies have been conducted to assess the strength of various numerical methods for wave structure interaction problems. For example, Ransley et al. (Ransley, Yan et al. 2019) led a comparative study of a range of numerical methods from low fidelity to high fidelity for focused wave interactions with a fixed structure. They pointed out that all methods involved perform well, while similar methods may present different capabilities. Then they further evaluated various numerical methods for the hydrodynamics of floating structures in focused waves (Ransley, Yan et al. 2020; Ransley, Brown et al. 2021). Their results show that the high-fidelity models can generally predict a better solution than the low-fidelity linear models. Bergua et al. (Bergua, Wiley et al. 2023) summarised the work done within the OC6 project and examined the capability of several numerical models for FOWT applications. In their study, several engineering codes and CFD codes have been applied to simulate the dynamic response of a 1:43 scaled version of a 3.6-MW wind turbine atop the TetraSpar floating support structure designed by Stiesdal Offshore Technologies under several load cases including wind only, wave only and combined wind and wave cases. In their results a reasonable agreement has been achieved for the prediction of the platform motion, but large differences exist among the models in the dynamic loading of the mooring lines, highlighting the uncertainties in setting up a numerical model for complex FOWT applications and the need for further code validation and verification exercises.

To systematically evaluate the performance of numerical approaches of varying fidelity for predicting the hydrodynamic response of the FOWT under both operational and extreme wave conditions, the 1st FOWT Comparative study (Ransley, Brown et al. 2022) as part of the EPSRC (UK) projects titled 'Extreme loading on FOWTs under complex environmental conditions' and 'Collaborative computational project on wave structure interaction(CCP-WSI)' was proposed. A series of load cases including the static equilibrium tests, free decay tests, operational and extreme focused wave cases were designed and tested experimentally for a 1:70 scale model of the UMaine VolturnUS-S semi-submersible platform (Allen, Viscelli et al. 2020). Given the availability of a large variety of numerical models including both Navier-Stokes and potential flow theory-based models as well as mesh-based and meshless methods, a 'semi' blind test approach has been adopted for the comparative study, in which 'simpler' test cases, i.e., free decay and wave only cases, were designed for validating a numerical model and the experimental results were made available to all the participants so they can refine the setup of their numerical models to achieve 'optimal' solutions based on users' experience with the specific model(s). This paper summarises the work submitted to the FOWT comparative study from a total of 17 contributions. The organization of the rest of this paper is as follows: the geometry and properties of the FOWT support structure and the setup of the experiments are provided in Section 2; Section 3 gives a brief description of each contributing code and its underlying numerical approach(es); in Section 4, for each test case the numerical results are compared with each other and against the experimental measurements with discussions on discrepancies in the results and their possible causes; a quantitative analysis of numerical errors against the experimental measurements is performed in Section 5; and the conclusions from the comparative study are drawn in the final section.

2. Problem definition and experiment setup

The FOWT model under consideration in the present study consists of a 1:70 scale model of the UMaine VolturnUS-S semi-submersible platform (Allen, Viscelli et al. 2020) and the turbine model based on the IEA 15MW reference wind turbine (Gaertner, Rinker et al. 2020). The geometry of this scale model differs slightly from the full-scale device. To retain approximately a scaling factor of the draft in the fresh-water basin, its mass properties are adjusted accordingly. Since the hydrodynamic response of the FOWT is the main focus of this study, the wind turbine aerodynamics is not modelled but the mass properties of the

rotor-nacelle-assembly as well as the tower are accounted for in the scale model.

The floating platform is made up of three outer columns with a diameter of 0.1778 m and a height of 0.5 m and one centre column with a diameter of 0.143 m. The distance between the outer and the central column axes is set as 0.7393 m. The tower with a height of 1.851 m is installed on the central column. Outer columns are connected to the central one at the bottom by pontoons with a dimension of 0.1778 m in width and 0.1 m in height, which are reinforced by three thinner braces at the top. The FOWT model is kept on station using a three-point mooring system constructed from '3mm long link' stainless chain. Due to the finite width of the working region, the laboratory moorings had to be truncated to fit the Ocean Basin. The mass properties and fairlead positions defined in the body-fixed coordinate system, and the mooring lines properties are provided in Tables 1 and 2 respectively.

The physical tests were conducted in the COAST Laboratory Ocean Basin at the University of Plymouth (Ransley, Brown et al. 2022), which is 35 m long and15.5 m wide. The water depth at the wavemakers is 4 m, while in the working area is 2.86 m. The detailed dimensions of this basin are provided in Fig. 1. At one side of this basin, 24 flap-type, force feedback-controlled wavemakers are used to generate waves at the water depth of 4 m. At the other side, a parabolic absorbing beach is facilitated as the relaxation zone to reduce the reflection of waves. A photo of the FOWT model in the wave basin is displayed in Fig. 2.

A number of load cases have been tested for the FOWT model, including the static equilibrium and free decay tests as well as the dynamic response under both operational and extreme focused waves. Static equilibrium tests involve two scenarios: one with and one without the mooring system attached, with the objective of isolating the effects of mooring lines. Table 3 shows the measured centre of mass (CoM) positions of the FOWT model with and without the moorings attached when in equilibrium. Three primary degrees of freedom (DoF): heave, surge and pitch are considered in the free decay tests. For each decay test, initial offsets of the centre of mass from the equilibrium position have been specified. The final load cases consist of a pair of unidirectional focused wave interactions with the FOWT. The waves are generated using the Edinburgh Designs Ltd wave synthesiser and paddle control software. The displacement of the paddles is calculated using linear wave maker theory. 112 components evenly spaced between frequencies of 0.15 and 2.0 Hz (spacing = 0.05/3 Hz) are supplied to the paddle control software based on a theoretical wave description. The two waves have similar steepness but vary in terms of peak frequency, Tp, and significant wave height, Hs. Both wave cases have a theoretical focus time, t_{focus} = 50 s, and a theoretical focus location in the global coordinate system, x_{focus} = 0 m, i.e., 17.3 m from the wavemakers. Table 4 summarises the theoretical parameters in the wave descriptions used for wave generation in two wave cases. For the focused wave cases, the surface elevations at nine different positions as defined in Table 5 are measured for both the empty tank case and when the FOWT model is present. Dynamic responses of the FOWT model under the two focused wave conditions are recorded. These provide a set of data for validating various aspects of the numerical models. For the full details of the experimental setup, description of the test cases and experimental resutls, readers are referred to the publication of Ransley, Brown et al. 2022.

Table 1
Mass properties and fairlead positions of the FOWT in the body-fixed coordinate system.

Items	Model values
Mass [kg]	56.3
Position of centre of mass (x, y, z) [m]	(-0.00477, 0.0, 0.26369)
Moments of inertia [kg·m²]	(26.68, 26.68, 14.18)
Fore fairlead position (x, y, z) [m]	(-0.83920, 0.0, 0.08571)
Aft-Port fairlead position (x, y, z) [m]	(0.41960, -0.72680, 0.08571)
Aft-Starboard fairlead position (x, y, z) [m]	(0.41960, 0.72680, 0.08571)

Table 2

Mooring line properties.

Items	Model values
Fore mooring length [m]	9.685
Aft-Port mooring length [m]	9.017
Aft-Starboard mooring length [m]	9.017
Dry mass/length [kg/m]	0.144
Submerged mass/length [kg/m]	0.125568
Mooring axial stiffness: [kN]	9.5335
Pretension: Fore, Port & Starboard [N]	7.6, 7.2

3. Numerical methods

In this comparative study, 17 contributions involving 30 research institutes have been received, of which 16 were presented at the 33rd International Society of Offshore and Polar Engineering Conference held in Ottawa, Canada between the 19th and 23rd of June 2023. The submitted results cover a range of numerical methods such as finite volume methods (FVM), finite element methods (FEM), boundary element method (BEM), spectral element method (SEM), and Smoothed Particle Hydrodynamics (SPH) for solving a hierarchy of free surface flow models based on the potential flow theory, Navier–Stoke equations and the hybrid between the two models. These include contributions from in-house codes, open-source codes, and commercial software. The mooring system is modelled either using a quasi-static method or a dynamic model. It is worth noting that out of the submissions, seven are based on different versions of OpenFOAM and its variants, two on Star-CCM+, and two on Orcaflex, which provides an opportunity to evaluate how numerical setups of the same or similar codes will affect the simulation results. The numerical model(s) applied within each submission are briefly described below and summarised in Table 6. For detailed specifics of each numerical model and its setup for the simulated test cases within the comparative study, readers are referred to the references attached to each code. In order to compare the different Navier–Stokes based models for modelling the more complex focused wave cases, details on the numerical setup of each model are provided in Table 7.

naoe-FOAM-SJTU (Xue, Zhang et al. 2023): The well validated in-house code naoe-FOAM-SJTU developed for solving marine hydrodynamics by Shanghai Jiao Tong University based on the open-source platform OpenFOAM is employed to perform the numerical simulations. The catenary line method is applied to model mooring line dynamics and two coordinate systems (the earth-fixed and body-fixed) are introduced to model the motion of the platform.

QaleFOAM (Jagdale, Li et al. 2023): The numerical model used in this comparative study is an in-house hybrid CFD model (QaleFOAM) coupled with the dynamic mooring model (MoorDyn). QaleFOAM is a domain decomposition model that combines the Quasi-arbitrary Lagrangian-Eulerian finite element method (QALE-FEM) in the far-field subdomain and a two-phase Navier–Stokes model (NS) solver OpenFOAM/InterDyMFoam in the confined near-structure sub-domain.

SEM (in-house code) (Visbech et al., 2024b): Motions are modelled in the time domain by solving the Cummins equations with mooring forces acquired from the discontinuous Galerkin SEM solver, MoodyCore, Palm et al. (2017). The linear pseudo-impulsive radiation problems are solved to provide frequency-dependent added mass and damping coefficients via a three-dimensional SEM-based solver. See Visbech et al. (2024a,b) for more details.

BFCS formulation (Zheng, Lei et al. 2023): The code directly solves the boundary-value problems and motions in the time domain using a consistent second-order model in the body-fixed coordinates following the structure's instantaneous position. The mooring system is approximated by equivalent linear stiffness coefficients. The drag loads on pontoons are considered by the KC-dependent drag coefficients. See Shao et al. (2022) and Zheng et al. (2023) for further details.

OpenFOAM (waves2Foam) (Zhou et al., 2023a): The multiphase

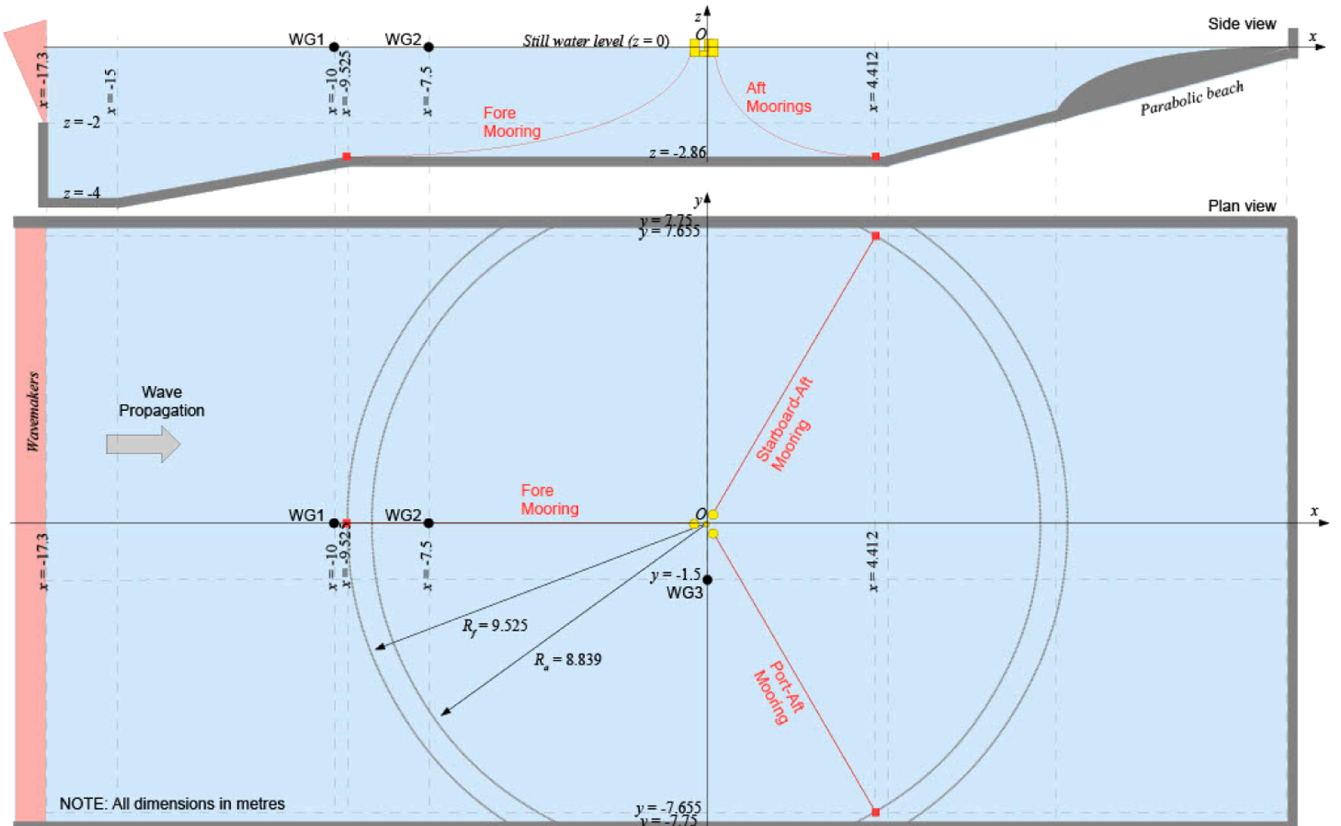**Fig. 1.** Dimensions of COAST Basin and definition of the global coordinate system [reproduced, with permission, from (Ransley, Brown et al. 2022)].
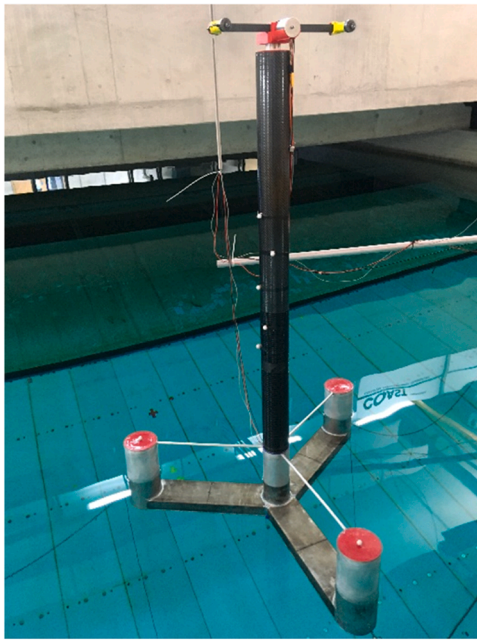
Fig. 2. 1:70 scale UMaine VolturnUS-S Semi-submersible Platform [reproduced, with permission, from (Ransley, Brown et al. 2022)].

Table 3
CoM position and pitch angle for the static equilibrium load cases.

	No moorings	With moorings
FOWT Comparative Study ID	FOWT1_EQ_unmoored	FOWT1_EQ_moored
Equilibrium CoM position [m]	(-0.00477*, 0.0*, -0.00126)	(-0.02038, 0.0, -0.02386)
Equilibrium pitch angle about CoM [°]	-1.729	-1.502

* these values are somewhat arbitrary for the unmoored case

Table 4
Focused wave conditions.

	Operational case	Extreme case
Water depth [m]	2.86	2.86
Theoretical peak period, Tp [s]	1.3831	1.9380
Theoretical significant wave height, Hs [m]	0.069	0.139
Theoretical focus phase, [°]	0	0

solver wave2Foam developed based on interFoam in OpenFOAM is used to solve viscous, incompressible, multiphase flows, where PIMPLE algorithm is adopted to deal with the velocity-pressure coupling. The dynamic mesh technique is utilized to realize the six degrees-of-freedom motion of semi-submersible platform. A built-in static catenary model is applied for the analysis of mooring line dynamics.

DIEGO (in-house code) (Peyrard, Benguigui et al. 2023): DIEGO is an aero-hydro-servo-elastic solver similar to engineering tools used by the industry for the FOWT structural design. It can be seen as a "low-fidelity" model, as it relies on simplified hydrodynamic assumptions (linear potential flow, Morison drag). The mooring lines are modelled by "cable" finite elements, which are linear elements with no rotation DoF (no bending, no torsion).

OpenFOAM (Barajas et al. 2024): OpenFOAM is used to create a numerical wave tank (NWT) to solve the FOWT response (the motion is defined by six degrees of freedom) under different loadings within the overset framework. The external library called MooDy is used for computing the mooring cable dynamics. This study uses the k-ω-SST turbulence model with the Larsen&Fuhrman enhancement to limit the overproduction of turbulence beneath surface waves.

STAR-CCM+ (overset) (Cui, Chen et al. 2023): The unsteady hydrodynamics of the FOWT support structure is simulated by using the overlapping grid method in the commercial CFD software STAR-CCM+ in which volume of fluid (VoF) method is adopted for capturing the free surface. The focused waves are generated based on the first-order linear superposition method and the quasi-static mooring line model is adopted for the analysis of mooring loads.

foamStar (Engel, Tierno et al. 2023): The numerical model is based on the coupling of a non-linear potential flow solver for the incident wave (HOS), a lumped-mass mooring dynamics model (Moordyn) and a CFD code named foamStar, based on OpenFOAM and developed by Centrale Nantes and Bureau Veritas.

OpenFOAM (AMI) (Zhou et al., 2023b,c): The OpenFOAM (Foundation Version 7) incompressible multi-phase solver "interDyMFoam" is utilised to perform all the simulations, in which the pressure velocity coupling is achieved through the PIMPLE algorithm. The built-in mesh generation tool "snappyHexMesh" and the arbitrary mesh interface (AMI) method are adopted to generate the computational mesh and to model the motion of the FOWT support structure.

MaPFlow (in-house code) (Ntouras et al., 2023): MaPFlow is a URANS solver developed at the NTUA. It is a cell centered solver that utilizes unstructured grids. For two-phase flows, the Volume of Fluid (VOF) method is employed coupled with an artificial compressibility formulation, see (Ntouras and Papadakis, 2020).MaPFlow is coupled with an in-house rigid body dynamics solver and with an in-house mooring line finite element solver, see Ntouras et. al. (2023).

MOST (in-house code), Orcaflex 1 and STAR-CCM+ (Niosi, Dell'Edera et al. 2023): MOST (in-house code) is a MATLAB-Simscape Multibody environment developed by MOREnergy Lab, Politecnico di Torino, analyzing multibody dynamics in floating wind turbines, accommodating concepts like wave energy converters. Like OrcaFlex, it numerically solves Cummins equation through Potential Flow Theory. The high-fidelity model in STAR-CCM+ uses Unsteady Reynolds Averaged Navier-Stokes equations and Scale-Resolving Hybrid turbulence model. In STAR-CCM+ and MOST, mooring forces are computed using Moordyn; Orcaflex uses its internal mooring solver.

OpenFOAM (v2006) (Eskilsson, Fernandez et al. 2023): Two-phase NS solver with a VoF approach from the OpenFOAM-v2006 finite volume framework. The model uses the modified mesh morphing approach of Palm & Eskilsson (2022). Turbulence is modelled by the k-omega-SST model with continuous wall functions (Menter et al., 2003). Mooring forces are provided by MoodyCore (Palm et al., 2017), a high-order discontinuous Galerkin model, using a one-way fluid-mooring coupling between the mooring and the CFD domain (Eskilsson & Palm, 2022).

OpenFOAM (v2106, waves2Foam) (Ransley, Brown et al. 2023): The two-phase, incompressible, RANS equations are solved using the VOF interface capturing method (Rusche 2002). Wave generation and absorption is achieved using relaxation zones (Jacobsen et al. 2012). Rigid body motion is accommodated via the 'mesh-deforming' method,

Table 5
Coordinates of wave gauges.

	WG1	WG2	WG3	WG4	WG5	WG6	WG7	WG8	WG9
x coordinate [m]	-10	-7.5	0	-0.4	-0.2	0	0.2	0.4	0.75
y coordinate [m]	0	0	-1.5	0	0	0	0	0	0

Table 6
Summary of software packages, numerical methods, mooring line models applied, and test cases conducted for the comparative study.

Code Name	Computational method	Solver	Mooring model	Test cases						
				Static equilibrium cases		Free decay tests			Focused wave cases	
				No moorings	With moorings	Heave	Surge	Pitch	Operational	Extreme
naoe-FOAM-SJTU (in-house code)	FVM	NS	Quasi-static	√	√	√	√	√	√	√
QaleFOAM (in-house code)	FVM/QALE-FEM	NS	Dynamic	√	√	√			√	√
SEM (in-house code)	SEM	PT	Dynamic	√	√	√	√	√		
BFCS formulation	BEM	PT				√	√	√	√	√
OpenFOAM (waves2Foam)	FVM	NS	Quasi-static		√	√	√	√	√	√
DIEGO (in-house code)	BEM	PT	dynamic ("cable" finite elements)	√	√	√	√	√	√	√
OpenFOAM	FVM	NS	Dynamic	√	√	√	√	√	√	√
STAR-CCM+ (overset)	FVM	NS	Quasi-static	√	√	√	√	√	√	√
foamStar	HOS/FVM	NLPT/NS	Dynamic	√	√	√	√	√	√	√
OpenFOAM (AMI)	FVM	NS	Quasi-static	√	√	√				
MaPFlow (in-house code)	FVM	NS	Dynamic	√	√	√	√	√	√	√
MOST (in-house code)	BEM	PT	Dynamic		√	√	√	√	√	√
Orcaflex 1	BEM	PT			√	√	√	√	√	√
STAR-CCM+	FVM	NS	Dynamic			√	√	√	√	√
OpenFOAM (v2006)	FVM	NS	Dynamic	√	√	√	√	√	√	√
OpenFOAM (v2106, waves2Foam)	FVM	NS	Quasi-static	√	√	√	√	√	√	√
OpenFAST	BEM	PT	Dynamic	√	√	√	√	√	√	√
Orcaflex 2	BEM	PT	Dynamic	√	√	√	√	√	√	√
WECSim	BEM	PT	Dynamic	√	√	√	√	√	√	√
DualSPHysics	SPH	NS	Dynamic (lumped-mass approach)						√	√

Table 7
Summary of the numerical setup for Navier-Stokes equation models (mesh based and SPH methods) for the focused wave cases.

Code Name	Mesh type	Domain dimension in x, y and z directions [m]	Boundary conditions (top, sides, bottom, wave generation, FOWT surface)	Cell/particle numbers, millions	Turbulence models
naoe-FOAM-SJTU (in-house code)	Unstructured	27.3, 9, 3.5	Open, slip, slip, velocity inlet, no-slip	2.4 – 3.48	k-ω SST
QaleFOAM (in-house code)	Unstructured	60, 15.5, 4.0 including the region of the potential flow	Open, slip, slip, paddle, no-slip	1.75 – 2.98	Laminar
OpenFOAM (waves2Foam)	Unstructured	35, 15, 4	Open, slip, slip, velocity inlet, no-slip	1.42	Laminar
OpenFOAM	Unstructured	35, 15.5, 6	Open, slip, slip, velocity inlet, no-slip	11.5	k-ω SST
STAR-CCM+ (overset)	Unstructured	27.5, 7.75, 5.72	Open, slip, no-slip, velocity inlet, no-slip	1.81	k-ω SST
foamStar	Unstructured	35, 15.5, 5.86	Open, slip, slip, velocity inlet, no-slip	1.81 – 5.98	k-ω SST
OpenFOAM (AMI)	Unstructured	9, 4, 4.59 for equilibrium and decay test cases only	Open, slip, slip, N/A, no-slip	2.23	Laminar
MaPFlow (in-house code)	Unstructured	35, 15.5, 2.86	Open, slip, slip, velocity inlet, no-slip	1.28 – 5.3	Laminar
STAR-CCM+	Unstructured	27.96, 8.66, 5.72	Open, slip, slip, velocity inlet, no-slip	3.3	Hybrid turbulence model
OpenFOAM (v2006)	Unstructured	30, 10, 5.72	Open, slip, slip, velocity inlet, no-slip	27.4	k-ω SST
OpenFOAM (v2106, waves2Foam)	Unstructured	7.75, 15.5, 5.72	Open, symmetric, slip, velocity inlet, no-slip	4.6 – 11	Laminar
DualSPHysics	Meshless	35, 3, 2.86	Dynamic boundary conditions	3.2	Laminar

based on the SLERP algorithm (Shoemake 1985), and the Newmark method (Newmark 1959). The mooring restoring force is simulated via a quasi-static model (Bruinsma et al. 2018).

OpenFAST (Holcombe, Edwards et al. 2023)**:** OpenFAST, is a coupled aero-hydro-servo-elastic engineering tool. The hydrodynamic model, HydroDyn, is a time domain tool, based on potential flow theory. QTFs are included, but only difference frequency QTFs. The additional global damping matrix is also applied, as with the other models, to represent viscous drag effects. In the structural model, all degrees of freedom are disallowed other than the six platform degrees of freedom. Mooring line characteristics are altered to account for the experimental mooring line lengths and density.

Orcaflex 2 (Holcombe, Edwards et al. 2023)**:** Linear hydrodynamic loads were modelled by solving the Cummin's equation in the time domain, using hydrodynamic coefficients from AQWA. Additionally, some non-linear hydrodynamic loads were included through the inclusion of full QTFs to model both wave drift and sum frequency loads, and an additional quadratic damping matrix to model viscous drag. Mooring lines were modelled in the time domain using lumped-mass modelling.

WECSim (Holcombe, Edwards et al. 2023)**:** Motions are modelled in the time domain by solving the Cummins equations with mooring forces acquired from the lumped mass model, MoorDyn (Hall et al., 2015). A global Morrison quadratic drag term is used to model viscous effects. In the edited model this term is reduced in proportion to the relative velocity between the fluid and structure to better capture the low frequency surge response caused by viscous drift (Holcombe et al, 2023).

DualSPHysics (Tagliafierro, Capasso et al. 2023)**:** DualSPHysics establishes a fluid-structure interaction environment based on SPH

([Domínguez et al., 2019];Domínguez et al. 2022). To reduce the basin size, the numerical flume for this application relies on an offline coupling that allows stepping 2-D wave-propagation information up to the full simulation using the MESH-IN technique (Ruffini et al., 2023). The catenary lines are resolved by the coupling implementation with MoorDynPlus (Martínez-Estévez, 2021), a reimplementation of Moor-Dyn (Hall et al., 2015).

4. Results and discussion

In the following sections, the relative performance of different models are compared and the results for the two distinctive groups of the Navier-Stokes equations and the potential flow theory are plotted together.

4.1. Static equilibrium tests

Before predicting the motion response of the FOWT model undergoing free decay and in waves, the static equilibrium test with and without the mooring restraints to find its stable positions in still water is simulated. Fig. 3 compares the predicted vertical (heave) and horizontal (surge) positions of the CoM as well as the pitch angle of the platform at the equilibrium state by both the numerical models and wave tank tests.

From Fig. 3 (a), it can be seen that for the equilibrium test without the moorings attached, most numerical models predict slightly higher vertical positions than the experimental result. Given the small magnitude of the equilibrium heave positions around the still water level and difficulties in measuring this in the wave basin, those results are considered satisfactory. However, it is clear that the results predicted by

the OpenFOAM, STAR-CCM+ (overset) and WECSim codes show a significant deviation from other results, and further analysis is required to find out the underlying causes. For the equilibrium test with the mooring restraint, again most numerical models predict a slightly higher heave position of the CoM compared to the physical measurement. Due to the restraints exerted by the mooring lines, most numerical models predict a lower equilibrium heave position for this case compared to the case without the mooring attached. However, the results from the naoe-FOAM-SJTU (in-house) code and Orcaflex 2 show an opposite trend, indicating problems in the numerical setup for this test case.

The surge equilibrium positions of the platform with moorings predicted by different numerical methods are shown in Fig. 3 (b). Compared to the experimental result, while all the predicted equilibrium surge positions are on the same side to the origin of the global coordinate system, they vary in magnitude. The results achieved by the naoe-FOAM-SJTU (in-house) code, QaleFOAM, OpenFOAM (v2106, waves-2Foam), and foamStar show a better agreement with the physical measurement.

Fig. 3 (c) shows the equilibrium pitch angle about CoM of the platform for both cases with and without moorings. While most numerical models predict a lower pitch angle than the experimental value especially for the case without mooring, the results are more consistent with each other than those of the predicted heave and surge positions. One exception is the result from the OpenFOAM (waves2Foam) model, where the predicted pitch angle is close to zero. Also, consistent with the experimental result, most numerical results predict a higher pitch angle for the no mooring case than the case with mooring attached.

Fig. 4 shows the mooring line tensions at fore and port-aft fairleads of the platform at equilibrium. While most numerical models have
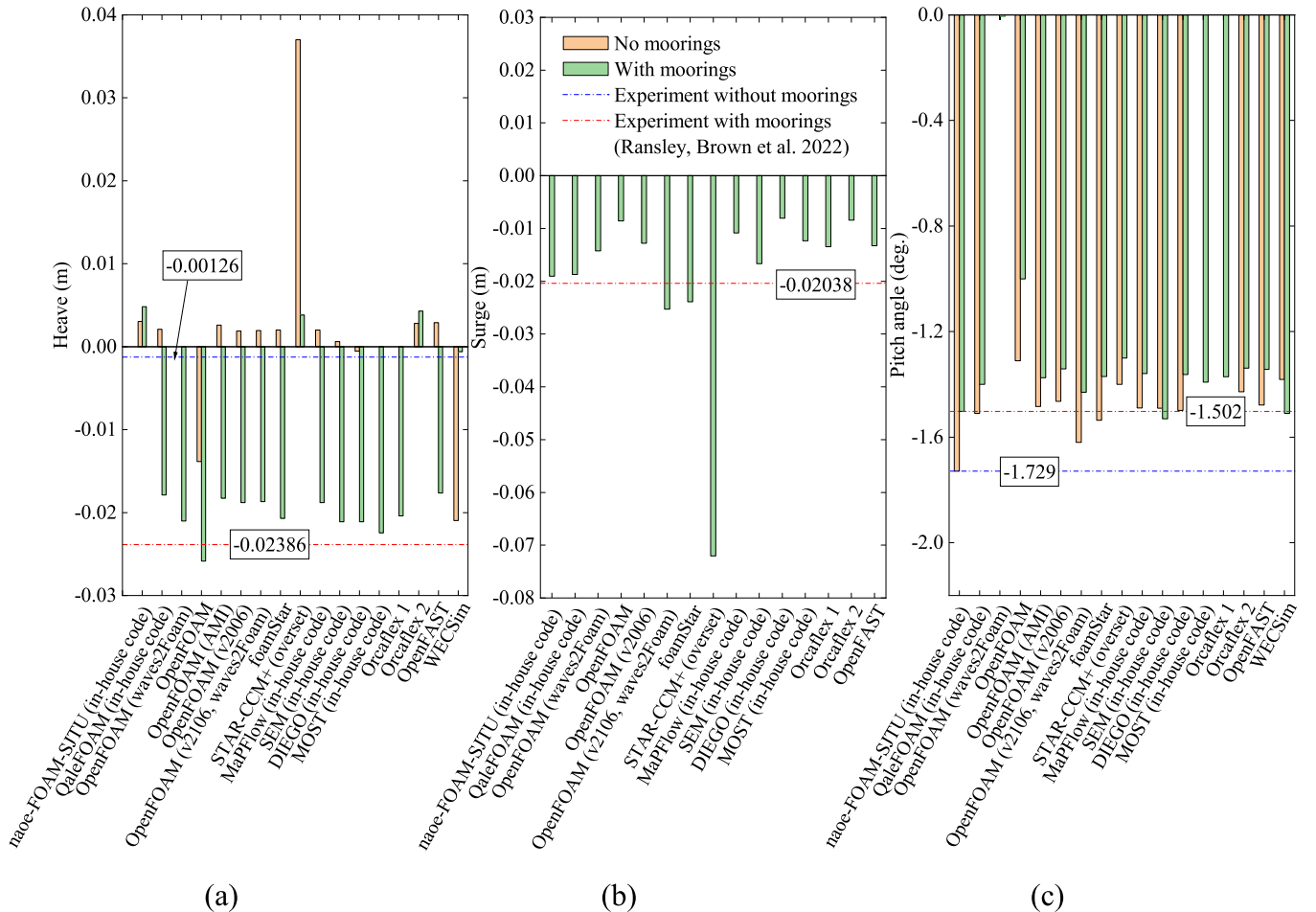

(a)   (b)   (c)

Fig. 3. Equilibrium position and pitch angle of the platform with and without the moorings.

underestimated the mooring line tension at the fore fairlead compared to the experimental result, better agreements have been achieved at the port-aft fairlead. One exception is the foamStar code, which has over-predicted the mooring loads at both fairleads and the results are closer to the fairlead's tension. As all the numerical results are quite close to each other, this shows that even a simplified mooring line model such as the quasi-static model will be adequate for this test case. Also, all numerical models predict a similar tension load at both port and fore-aft fairleads, which is in contrast with the experimental results in which the mooring load at the fore fairlead is higher than that at the port-aft fairlead.

Comparing the performance of potential theory and NS equations-based models it can be concluded that for this test case both models are capable of predicting reasonable and comparable results. This is expected as viscous effects will not be important when the FOWT model reaches its equilibrium position. Also, as differences exist even among the results from the same or variants of the same numerical models, e.g., OpenFOAM, it can be conjectured that main reasons for the discrepancies in the numerical results are due to the different numerical setup of both flow and mooring line models as well as numerical errors in the solutions. For the differences between the numerical results and the experimental data, as discussed in Ransley, Brown et al. 2023, a possible reason is the underestimation of the FOWT model mass in the description (Table 1).

4.2. Free decay tests (in heave, surge and pitch)

Once the equilibrium position of the moored FOWT model is determined, the free decay tests in heave, surge, and pitch are simulated based on the specified initial offset in each degree of freedom.

The time history of the heave motion of the system from the heave decay test is displayed in Fig. 5 (a). The predicted heave displacements by the numerical models generally agree well with each other and with the experimental measurement, especially for the first few oscillation cycles. It can be observed that some results, e.g., from SEM (in-house), DIEGO (in-house), MOST (in-house) and Orcaflex 1 codes underpredict the amplitude of the first peak while the result from STAR-CCM+ (overset) shows a substantial phase shift.

A similar trend can be observed for the surge motion response from the surge decay test in Fig. 5 (b), and a noticeable discrepancy can be

found between the results of STAR-CCM+ (overset) and other numerical results and the experiment. This discrepancy might result from the iterative error accumulating in the computational process of solving the quasi-static catenary model due to the large surge motion stroke (Cui, Chen et al. 2023).

The results for the pitch decay test are shown in Fig. 5 (c). While most results exhibit a similar trend in the predicted oscillation amplitudes, noticeable discrepancy can be found in the predicted oscillation phases. This, along with the strange result of OpenFOAM (waves2Foam) and the large deviations in the results of naoe-FOAM-SJTU (in-house), highlights the challenges in correctly setting up a numerical model for predicting the pitch response of the FOWT model.

To quantify the comparison among the numerical results, both the predicted natural periods and damping ratios are calculated from the submitted data and are compared with the experimental result. Fig. 6 shows a comparison of natural periods of the floating platform in heave, surge, and pitch decay tests from different numerical methods. Since different submissions have different time ranges in the three degrees of freedom motions, the first five cycles of the free decay time history are used to calculate the natural periods. Based on the results, it can be concluded that while the natural periods of the heave response are well predicted by most numerical models, some numerical models slightly overestimate the natural periods of the surge response compared to the experimental results and at the same time most models slightly under-predict the natural periods of the pitch motion. Again, the differences in the results may be due to the setup of the numerical model and no clear link to the selection of mooring line models can be established.

The damping ratio is calculated based on the logarithmic decrement method, which can be given by (Casiano 2016)

$$\zeta = \frac{\lambda}{\sqrt{4\pi^2 + \lambda^2}}$$

where λ is the logarithmic decay rate, the formula of which is as follows (Joo 2016)

$$\lambda = -\frac{1}{i \cdot T} \ln \left(\frac{A(i)}{A_0} \right)$$

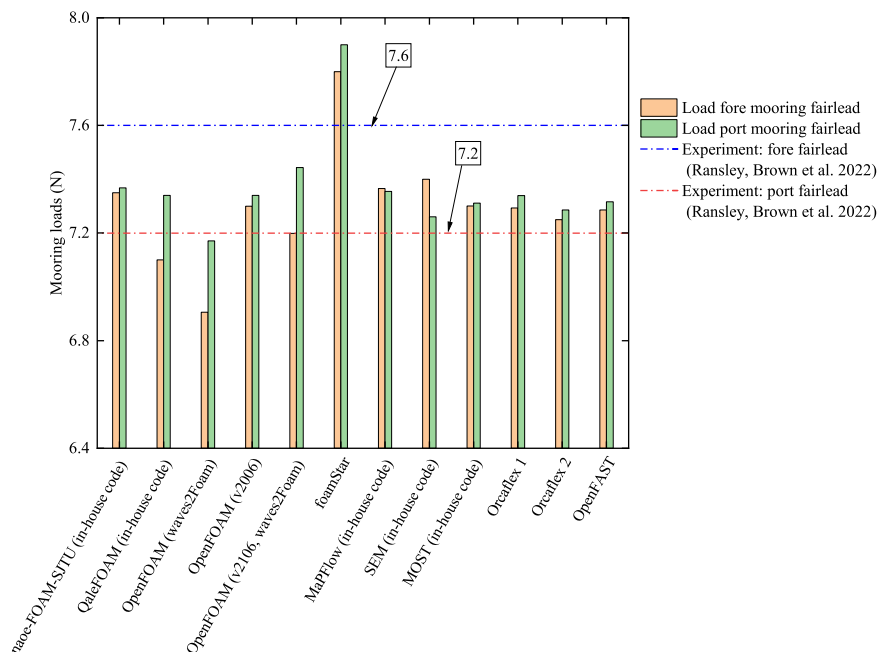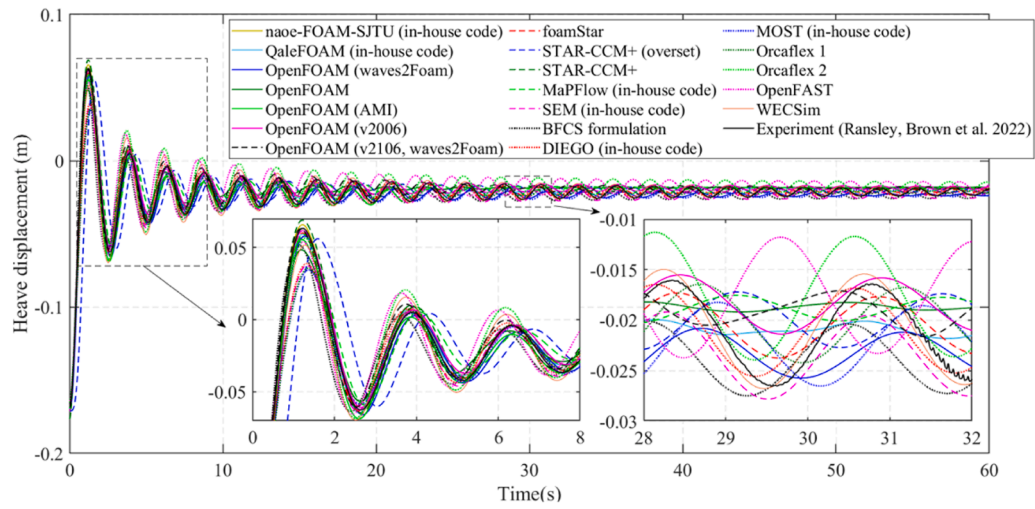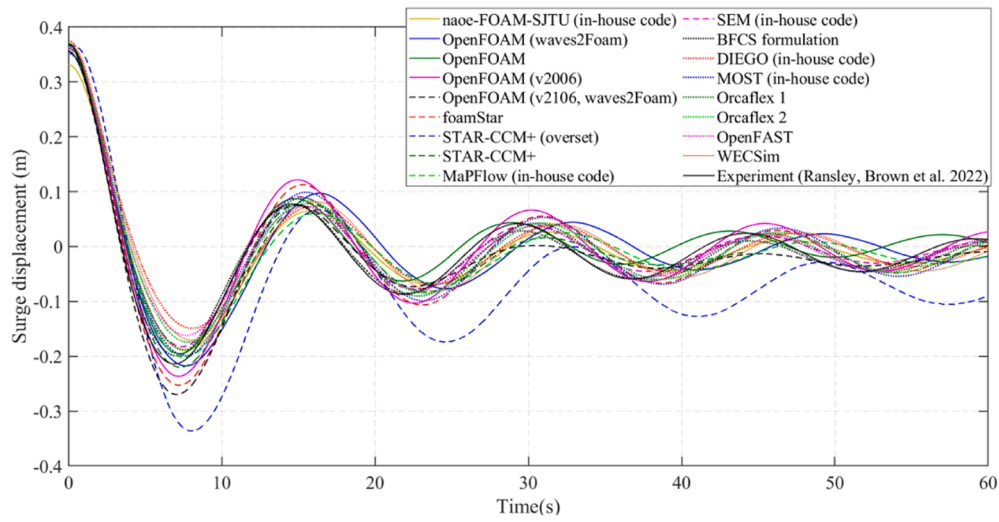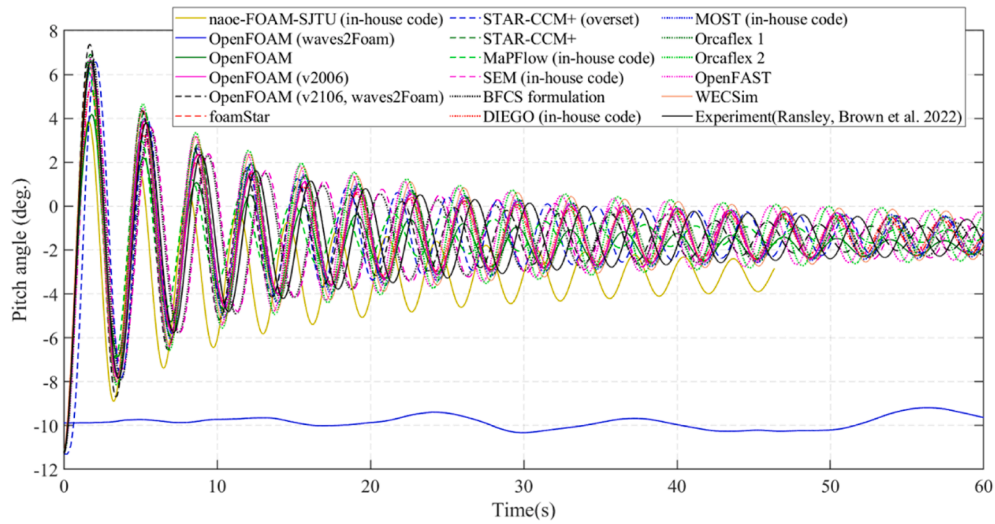where T [s] is the period of the damped oscillations, which is the same as

Fig. 4. Mooring loads of the platform with the mooring system when in equilibrium.

(a) Heave displacement from the heave decay test

(b) Surge displacement from the surge decay test

(c) Pitch angle from the pitch decay test

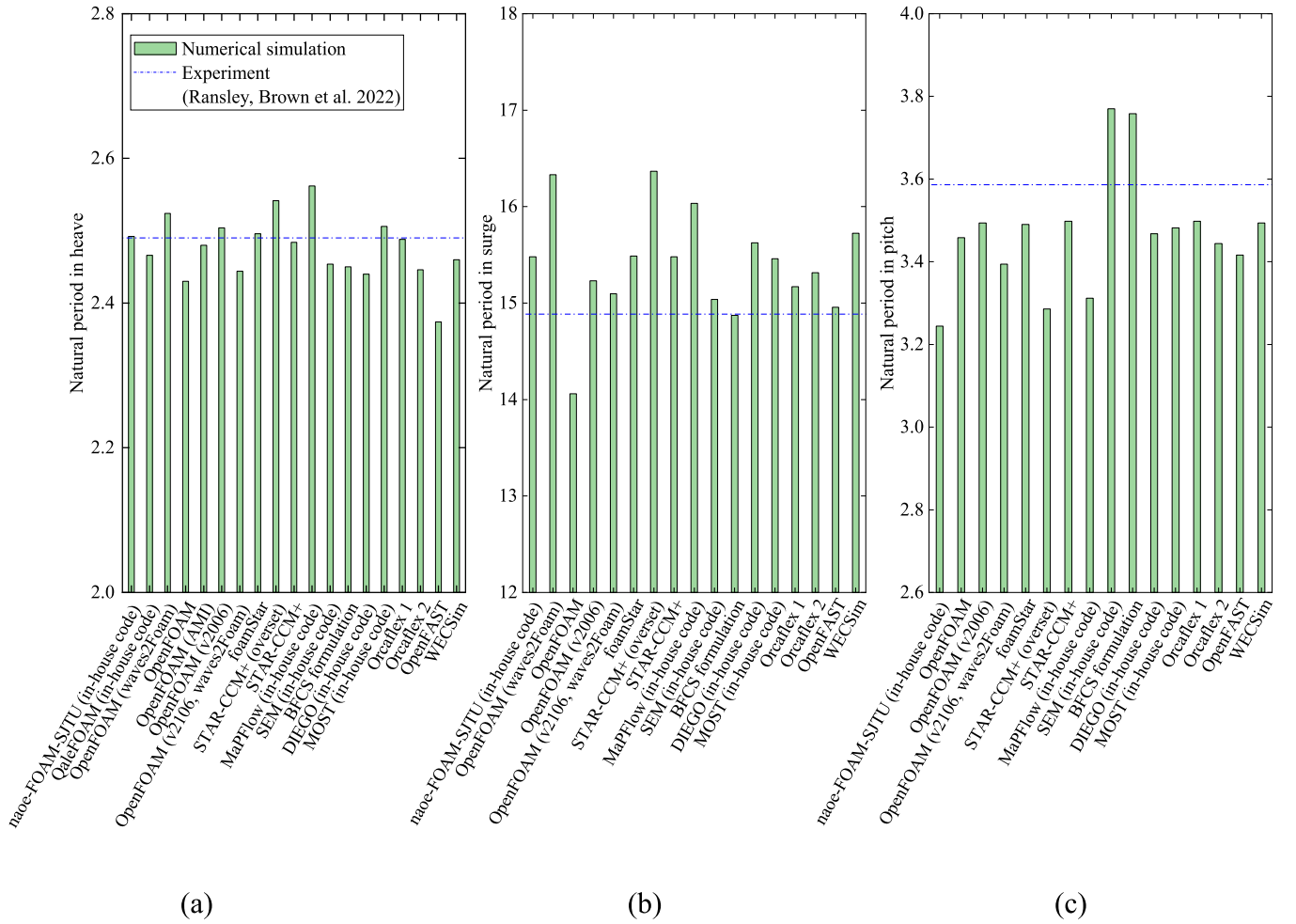**Fig. 5.** Free decay motion of the floating platform.

Fig. 6. Natural periods of the platform in heave, surge, and pitch from the heave (a), surge (b), and pitch (c) decay tests, respectively.

the natural period in the present study. A_0 [m] is the initial amplitude of oscillation, and $A(i)$ [m] is the ith peak amplitude.

Based on this method, the damping ratios from the free decay tests are calculated. Fig. 7 shows the comparison of damping ratios among numerical methods for the heave, surge, and pitch decay tests and against the experimental results. It can be seen that the damping ratios show much wider variations among the numerical models. For the heave decay test, SEM (in-house), OpenFOAM, MOST (in-house) and Orcaflex 1 predict much lower heave damping ratios than the experimental value. Substantially large damping ratios have been predicted by STAR-CCM+ and OpenFOAM (v2106, waves2Foam) for the surge decay and by naoe-FOAM-SJTU (in-house), OpenFOAM, and MaPFlow (in-house) for the pitch decay, while OpenFAST, Orcaflex 2, and WECSim (all based on the potential flow theory) consistently underpredict the pitch damping ratio. Generally, Navier-Stokes based models can predict better damping ratios especially in the pitch motion than the potential flow based models. PT models are much more efficient, but rely on proper calibration of the damping terms.

Fig. 8 shows the comparison of the mooring loads at fairleads of the fore and port-aft mooring lines based on the submitted mooring load data for the decay tests. It can be observed that the results from the WECSim model exhibit substantial oscillations at the beginning of the simulation indicating large dissipation in the numerical scheme. However, this does not appear to influence the subsequent results. On the other hand, substantially low mooring load values have been predicted initially by the STAR-CCM+(overset) model, which are then recovered to more normal values after one second of the simulation.

Most numerical models predict a similar trend to the experiment for the mooring line tensions at both fairleads in the heave decay test, with the exception of the results of QaleFOAM (in-house) and foamStar, which overpredict mooring line tensions. The numerical code Open-FOAM (waves2Foam) tends to underpredict the heave response compared to the experimental test.

Similar to the heave decay test, most numerical models accurately capture the mooring load at the fore fairlead mooring line in the time range plotted for the surge decay test. However, greater discrepancies of the mooring load at the port-aft fairlead among numerical models can be identified, and in particular foamStar and STAR-CCM+ (overset) codes have overestimated the mooring load at the port fairlead. In general, these numerical models can reasonably capture the characteristics of mooring line loads in the surge decay test.

For the pitch decay test, it is found that most numerical models tend to predict a similar trend for the mooring line load at both fairleads. However, the mooring line tensions by the foamStar and OpenFOAM (waves2Foam) codes differ significantly from the physical measurements and other numerical models. For example, the mooring line tensions at both the fore and port fairleads are considerably overestimated by the numerical model from foamStar.

It might be worth noting that for the free decay tests, when a solution reaches the steady state, the positions of the platform and mooring loads should be the same as those in the static equilibrium tests. Most models have achieved consistent results in this respect but with a few exceptions, highlighting the importance of consistency in the setup of a numerical model.
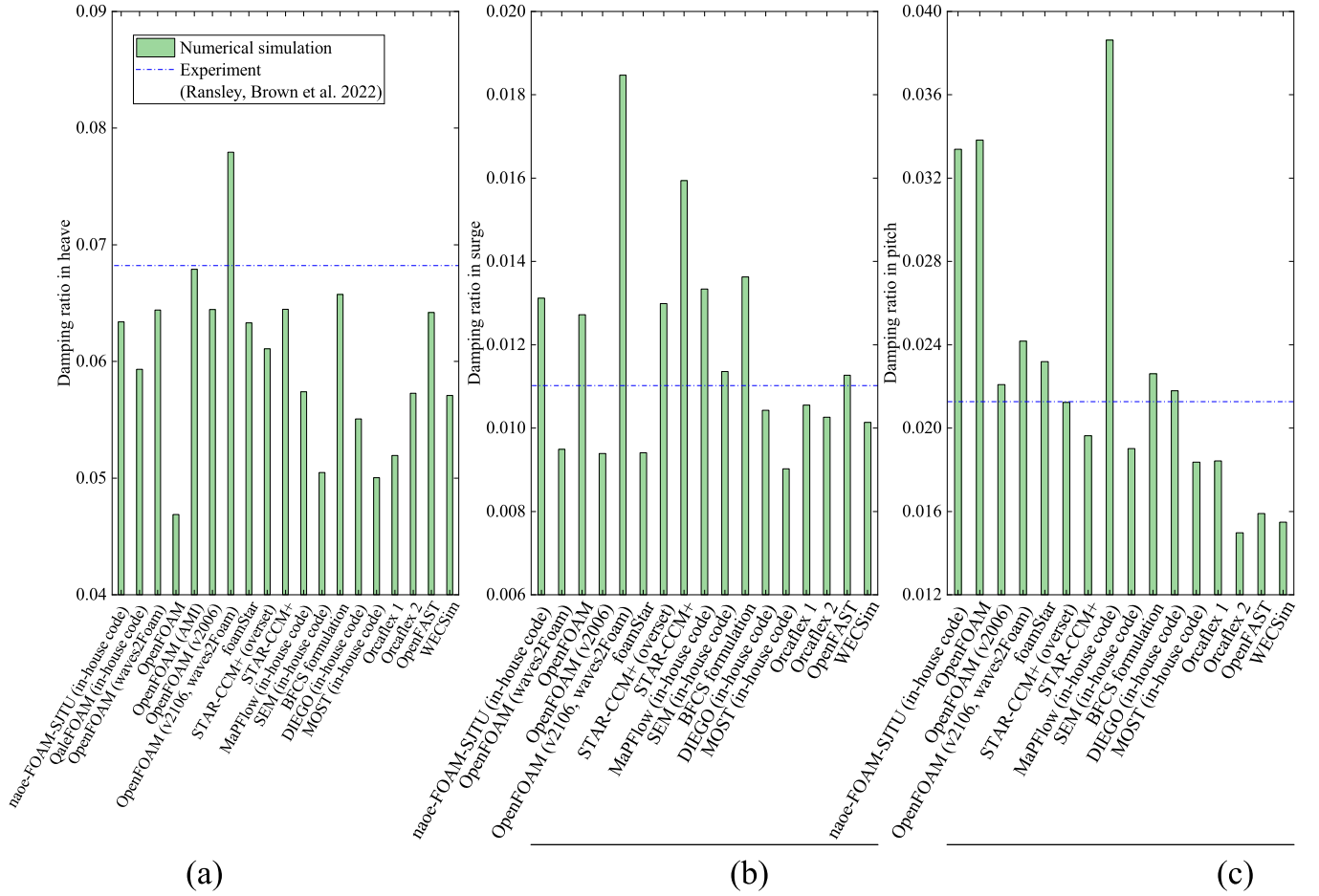
Fig. 7. Damping ratios of the platform in heave, surge, and pitch from the heave (a), surge (b), and pitch (c) decay tests, respectively.

4.3. Focused wave cases (operational and extreme)

Before modelling the dynamic response of the floating platform under both operational and extreme focused wave conditions, the generation and propagation of focused waves in an empty tank are simulated first.

Fig. 9 shows the free-surface elevations predicted by numerical models along with the experimental measurements at probes WG 4, 6 and 8 for both focused wave cases. The probe WG 6 is located at the origin of the global coordinate system, and probes WG 4 and WG8 are located before and after the origin, respectively. The results demonstrate that most numerical models have reproduced the focused wave groups reasonably well and they are in good agreement with the experiments for these probes, especially for the operational focused wave case. However, it is found that there are noticeable variations in the numerical results. For example, for the operational focused wave case, the wave amplitudes before and after the main crests predicted by the STAR-CCM+ (overset) code are slightly larger than other numerical results and the experimental result. For the extreme focused wave case, the Dual-SPHysics code slightly underpredicts the peak value and OpenFOAM underpredicts the wave amplitudes after the main peaks. The naoe-FOAM-SJTU (in-house) code, which used the JONSWAP wave spectrum rather than the experimental PM wave spectrum to generate the waves, overpredicts the wave amplitudes both before and after the focal point and exhibits a large phase difference from the other results.

The time history of the surface elevation for the probe WG6 is further analysed with fast Fourier transform (FFT) method to obtain the power spectrum density (PSD), which is calculated over the range of [40.5–54.5] s and displayed in Fig. 10. It confirms that most numerical

methods can reproduce the waves reasonably well since the PSD obtained by these methods are basically in agreement with each other and that of the experiment, despite minor discrepancies in the PSD magnitude and minor oscillations at higher frequencies from the STAR-CCM+ (overset) model. But for the extreme focused wave case, a very large peak PSD value at the peak frequency is predicted by the naoe-FOAM-SJTU (in-house) in Fig. 10 (b), as a result of a different wave spectrum that has been used for generating the focused waves by the model.

Fig. 11 illustrates the dynamic response of the platform in heave, surge and pitch degrees of freedom under the condition of the operational focused waves. To further examine the motion responses of the platform in these three degrees of freedom, the power spectrum density in the frequency space (based on the time range of [40.5–54.5] s) is plotted in Fig. 12.

For the heave motion in the time domain (Fig. 11 (a)), it can be observed that compared to the physical measurements, most numerical models start with a higher (predicted) equilibrium heave position as discussed in section 4.1 and some models (for example QaleFOAM (in-house), STAR-CCM+ (overset), foamStar, Orcaflex 1, STAR-CCM+, WECSim and its modified code) experience noticeable oscillatory heave motions due to the fact that the initial position of the FOWT model is not at equilibrium. Despite the discrepancies in the initial heave position, the prediction of the heave motion by most numerical models agrees reasonably well with the experimental results, particularly in the main crests and troughs around the focal point. When viewing the frequency domain, two distinct peaks at the peak wave frequency and the heave natural frequency respectively can be found, and most results can capture these two peaks well, except for the results of BFCS formulation, OpenFOAM and OpenFOAM (v2006). It is found that for the BFCS
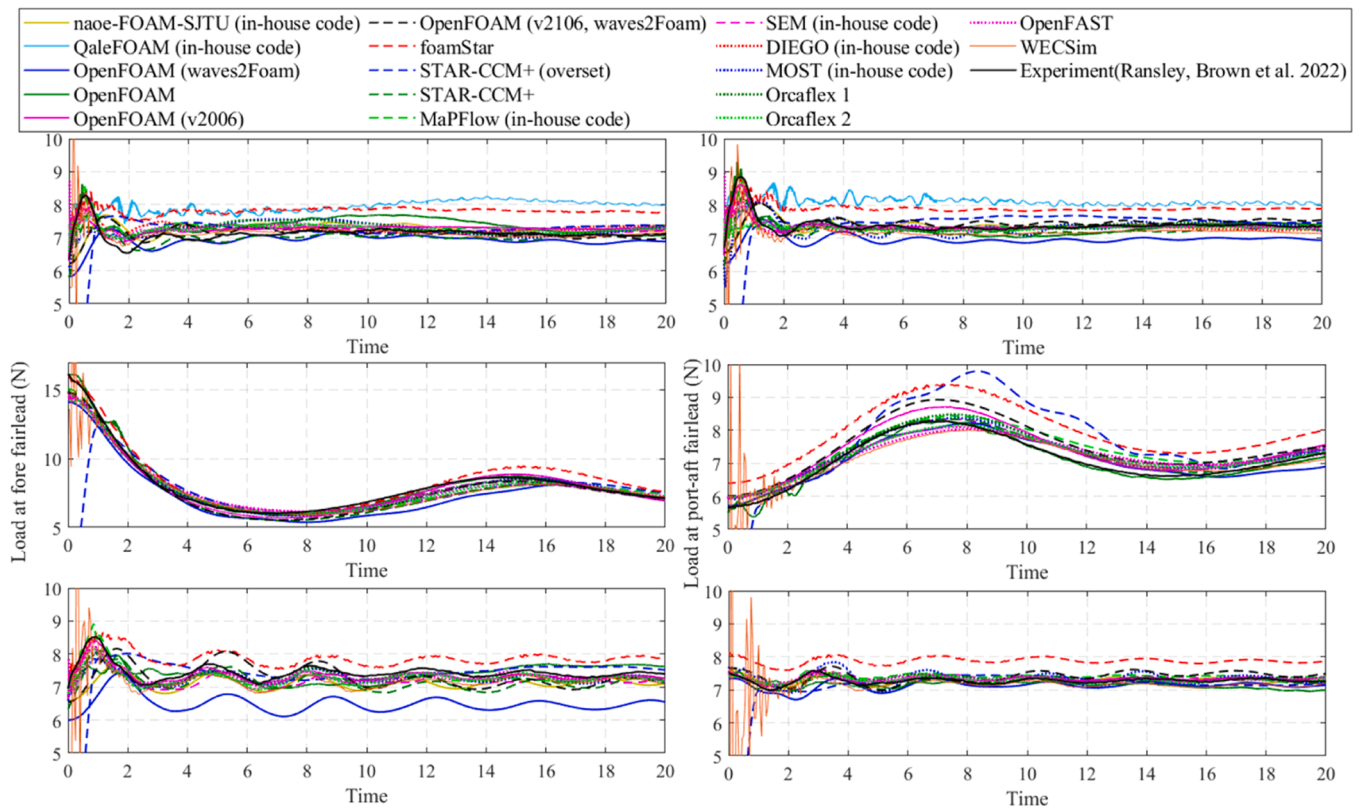
Fig. 8. Mooring loads from the free decay tests at the fore fairlead (left column) and the port-aft fairlead (right column): top row: heave decay; middle row: surge decay; bottom row: pitch decay.

formulation, while it can capture the peak wave frequency, the distribution of the PSD is spread to a wider area and the peak at lower frequency is also shifted to the right from the heave natural frequency. For the OpenFOAM and OpenFOAM (v2006), they obviously underpredict the peak at the wave frequency. On the other hand, the results of foamStar overpredict the peak at the heave frequency, which might be attributed to the larger motion of the floating platform at the beginning. The MOST (in-house) based on WECSim predicts a good value at the wave frequency while Orcaflex 1 and STAR-CCM+ slightly overpredict and underestimate it, respectively. From these results, it seems that a properly adjusted linear model might produce better results than a high-fidelity model. OpenFOAM (v2106, waves2Foam) simulates a greater amplitude peak response around the wave frequency, and unmatched trends are found at lower frequency from WECSim's results. Little difference is found between OpenFAST and Orcaflex 2

Compared to the heave case, the surge motion in the operational focused wave case seems to spread more considerably among the different numerical models. There are noticeable discrepancies in the quality of predicting the surge displacement by numerical models, especially before and after the main wave crests. Specifically, the drift motion (Ma and Yan 2009) after the focused time is observed in most numerical models. Generally, the NS solvers predict the surge motion well since the non-linear effects are considered. However, the Qale-FOAM (in-house) code predicts a delayed response in the drift motion. It seems that the STAR-CCM+ (overset) predicts a premature surge motion relative to the experimental test, possibly due to the simulation not starting at the equilibrium position in surge. The result of the Open-FOAM (v2106, waves2Foam) shows a strange surge response before the focusing time. Most linear models such as those from MOST (in-house), Orcaflex 1 and WECSim do not capture the drift motion well, while the modified WECSim code predicts a comparable drift motion with the experimental test. In the frequency domain, the surge motion of the platform can be seen in the low frequency range. However, there exist

significant discrepancies in the predicted main peak among different numerical models. It is also found that a very small response around the surge frequency has been predicted from the numerical code of Orcaflex 1.

Most numerical models tend to predict the pitch motion well in main wave crests while displaying greater differences between each other and from the experimental data in other phases. Again, due to the simulation not starting at the equilibrium position in pitch, some numerical models such as those based on QaleFOAM (in-house), STAR-CCM+ (overset), WECSim, and its modified code predict relatively large pitch motions before the arrival of the focused wave train. It also can be seen that the OpenFOAM seems to produce some odd pitch motion and differs noticeably from both the experimental results and other numerical solutions. These results might be a consequence of the coupling methodology used to save computational time and resources (waves are generated and propagated in a two-dimensional mesh and then, in the vicinity of the FOWT, mapped into a three-dimensional mesh), in which secondary motions are not well captured. In the frequency domain, it is evident that the numerical models based on QaleFOAM (in-house) and OpenFOAM overpredict the peak at the pitch natural frequency. Some curious motions at lower frequency are observed, possibly due to the coupling of different degrees of freedom motions. In addition, the incorrect pitch motions predicted by the OpenFOAM are evidenced by the greater discrepancy in the frequency domain from others.

Fig. 13 shows the response of the floating platform in heave, surge, and pitch when it is subjected to the excitation of extreme focused waves. The power spectrum density in the frequency space (also based on the time range of [40.5–54.5] s) is also provided in Fig. 14.
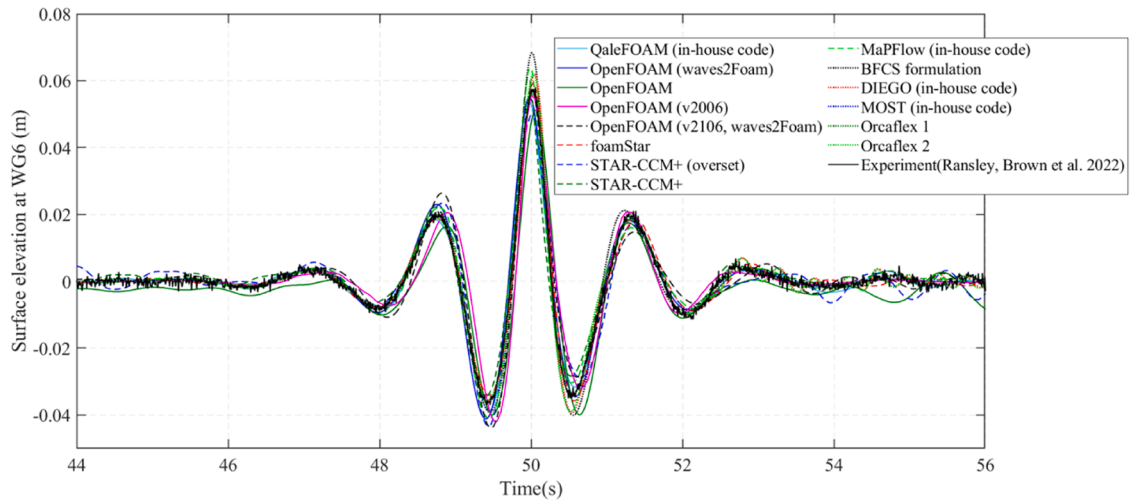
In such wave intensity cases, most numerical solutions generally tend to reproduce the heave response well compared to the experiment. However, clear discrepancies among the results can be observed. The amplitude of the heave response before the focal time is overestimated by the numerical solution of naoe-FOAM-SJTU (in-house) code. For the
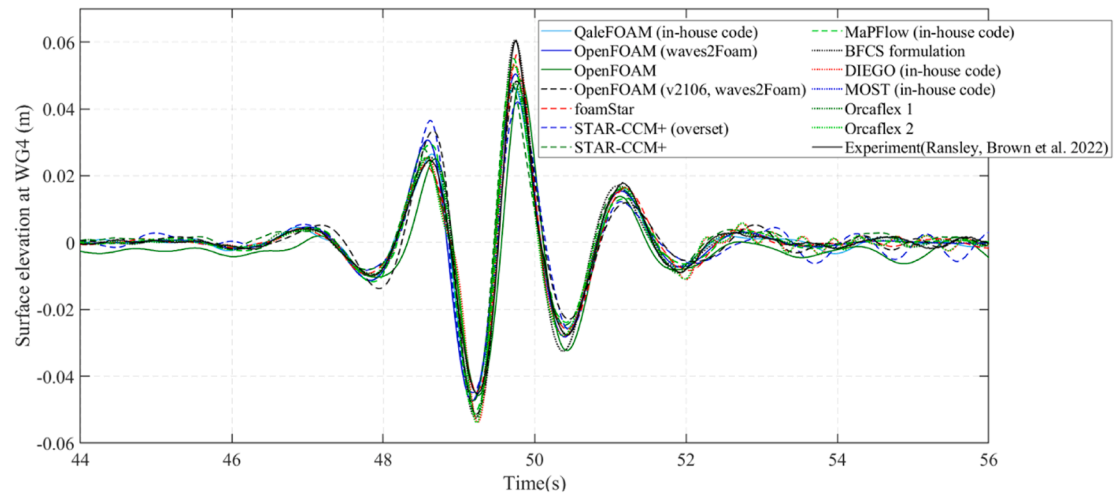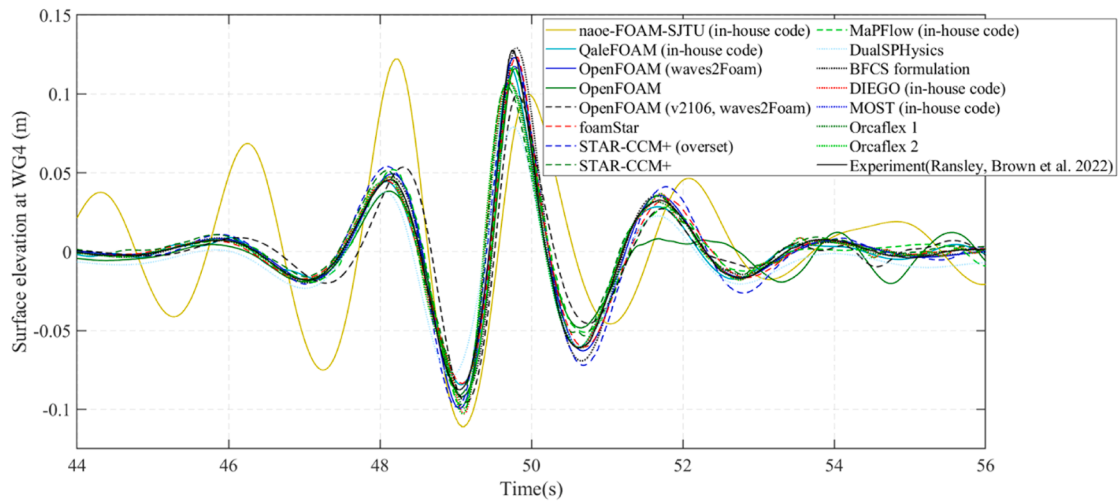
Fig. 9. Surface elevation measured at WGs 4, 6 and 8 from an empty tank test for focused wave cases: (a), (c) and (e) operational case and (b), (d) and (f) extreme case.
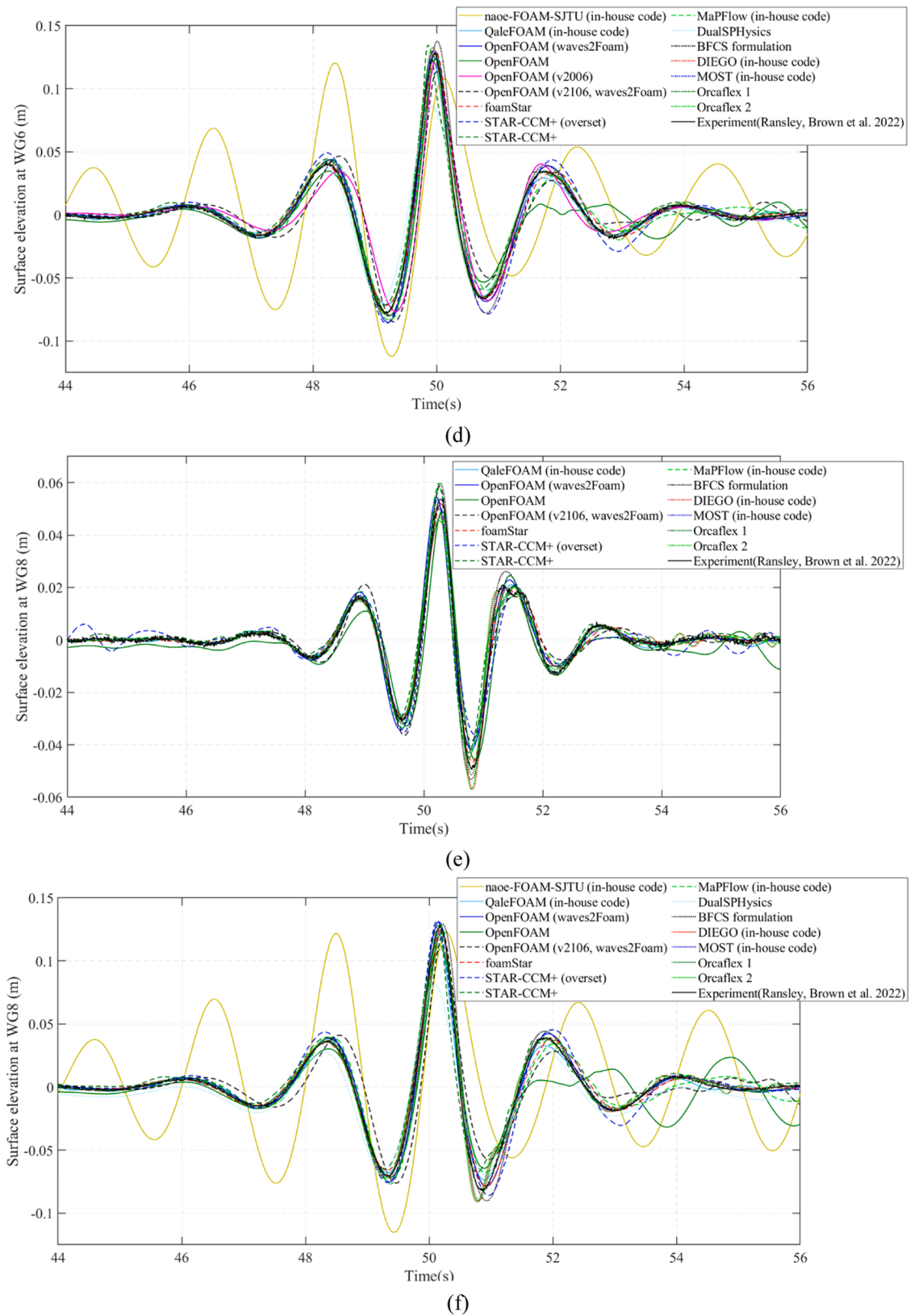
(d)

(e)

(f)

Fig. 9. (*continued*).

OpenFOAM result, while it overpredicts the peak heave response, the solution damped out much quicker than other results. The STAR-CCM+ (overset)code significantly underestimates the heave displacement throughout the duration of the simulation. In the frequency domain, a large discrepancy of results between the results of naoe-FOAM-SJTU (in-house) code and other numerical models and the experiment can be observed. For fair comparison across all numerical models, the results of naoe-FOAM-SJTU (in-house) code are not displayed here. Similar trend
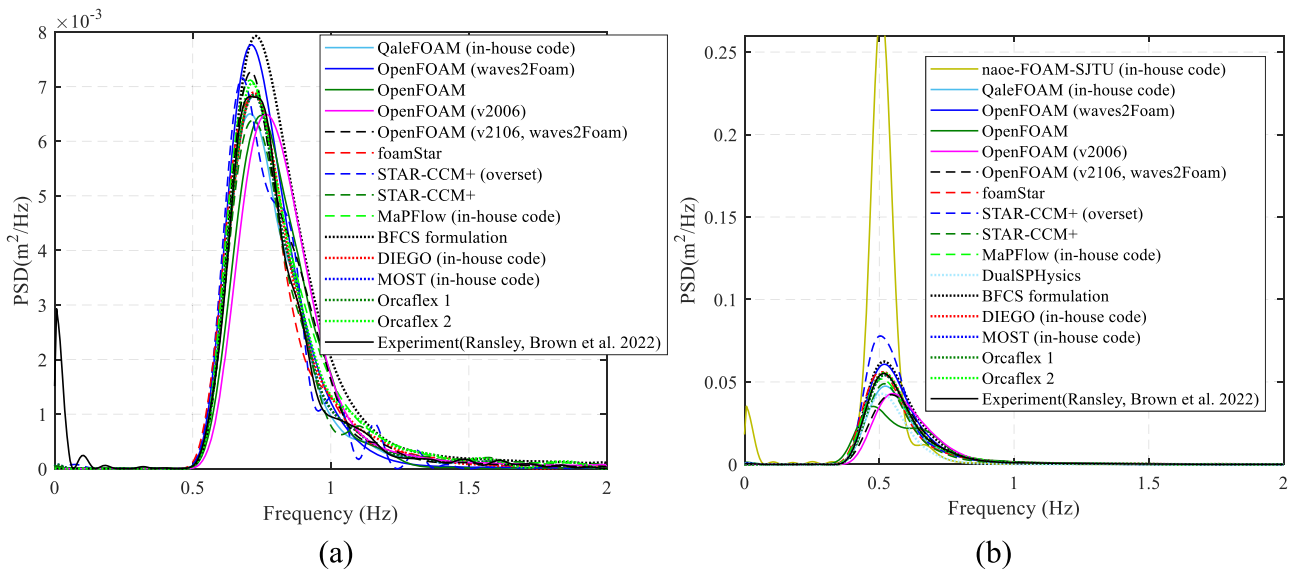
Fig. 10. PSD per frequency of surface elevation at WG6 from an empty tank test for focused wave cases: (a) operational and (b) extreme (over the range of [40.5 – 54.5]s).

is also observed in the results by OpenFOAM. STAR-CCM+ (overset) evidently underestimates the response around both wave and heave natural frequencies and has noticeable disparities at higher frequencies.

There appears to be more variations in the predicted surge motion of the floating platform by the numerical models compared to the heave motion, especially before and after the main crests. Specifically, significant discrepancies are found in naoe-FOAM-SJTU (in-house) code and QaleFOAM (in-house) code, as the former code entirely overpredicts the surge motion and seems to fail to capture the drift motion after the focused time, and the latter overestimates the surge motion both before and after the main crests. DualSPHysics underestimates the surge displacement and experiences a lower amplitude of drifting movement. Linear models of MOST (in-house), Orcaflex 1, STAR-CCM+, OpenFAST, Orcaflex and WECSim tend to slightly underestimate the surge displacement. WECSim seems to predict a shorter drift motion and its modified model predicts a comparable drift motion to the experimental result. In general, the NS solvers can predict a better surge motion. In the frequency domain, noticeable discrepancies at higher frequency by the naoe-FOAM-SJTU (in-house) code are observed. From the frequency analysis, some issues in results of the numerical model by OpenFOAM can be identified, as large disparities are found at both lower and higher frequencies. On the other hand, MOST (in-house), Orcaflex 1, Open-FAST, Orcaflex and WECSim predict a very small response around the platform surge frequency (low frequency).

Similar to the surge motion response, the floating platform has a large motion in pitch degree of freedom before the arrival of the focused waves in the results of the QaleFOAM (in-house) code. This is mainly due to the fact that the initial position of the FOWT model is not at equilibrium in pitch and surge directions. An odd phenomenon in the pitch motion is observed in OpenFOAM's solution, similar to the operational wave case. The almost same pitch motion at main peak has been predicted by MOST (in-house) and Orcaflex 1, but the pitch response tends to be damped out quickly when the extreme focused wave has passed. Compared to OpenFAST and Orcaflex 2, WECSim and its updated model predict a comparable pitch angle response to the experimental test after the interaction with the extreme focused wave despite a phase shift. In general, most numerical models can predict the pitch response well as far as the main wave crests are concerned. When viewing the results in the frequency domain, relatively large difference in frequency content between some numerical models (for example, naoe-FOAM-SJTU (in-house), QaleFOAM (in-house), OpenFOAM, and

DualSPHysics) and the experiment test are observed. It seems that the larger pitch motion before the main crests observed in the time domain results in the differences in the frequency domain. The odd behaviour in the pitch motion of the OpenFOAM's model is also reflected in its frequency distribution. The numerical model from DualSPHysics fails to match the lower frequency and overpredicts the higher frequency content. However, these numerical models reasonably simulate the pitch response frequency and wave frequency. It is also found the occurrence of four distinct peaks at different frequencies among most numerical results and in the experimental measurement, which correspond to frequencies at the surge natural frequency, the heave natural frequency, the pitch natural frequency, and the wave frequency, respectively. It indicates that the pitch response is also related to the responses in other degrees of freedom (i.e., coupling effects from different motion responses).

Fig. 15 shows comparison of mooring line tensions at the fore and port fairleads among different numerical solutions. The general variation of mooring loads with the time is similar to that of surface elevation and heave motion both for the operational and extreme focused wave cases. This indicates that mooring line tensions of the system are dominated by the heave motion. Clearly, there are systematic offsets in the mooring loads by most numerical models in the operational focused wave case. Despite this, the predicted mooring line tensions are reproduced reasonably well during the passing of the main wave train. In both operational and extreme focused wave cases, some models predict unsteady mooring loads at both the fore and port fairleads before the arrival of the focused waves, and the mooring loads predicted by the OpenFOAM model show large oscillations throughout the simulation.

Fig. 16 displays mooring loads in the frequency domain for both the operational and the extreme focused wave scenarios. Most numerical models properly reproduce the expected frequency but tend to slightly underestimate the higher frequency content of the mooring loads both at the fore and port fairleads under these two focused wave cases. The dynamic loading of mooring lines among different numerical methods has a significant spread, which might be relative to different inertial forces endured in different platform motions in the heave, surge, and pitch degrees of freedom (Bergua, Wiley et al. 2023). When the floating is subjected to the operational focused wave, it can be clearly seen that MOST model overpredicts the mooring load at the port fairlead at higher frequency. Under the extreme focused wave conditions, naoe-FOAM-SJTU (in-house) and MOST (in-house) codes overpredict
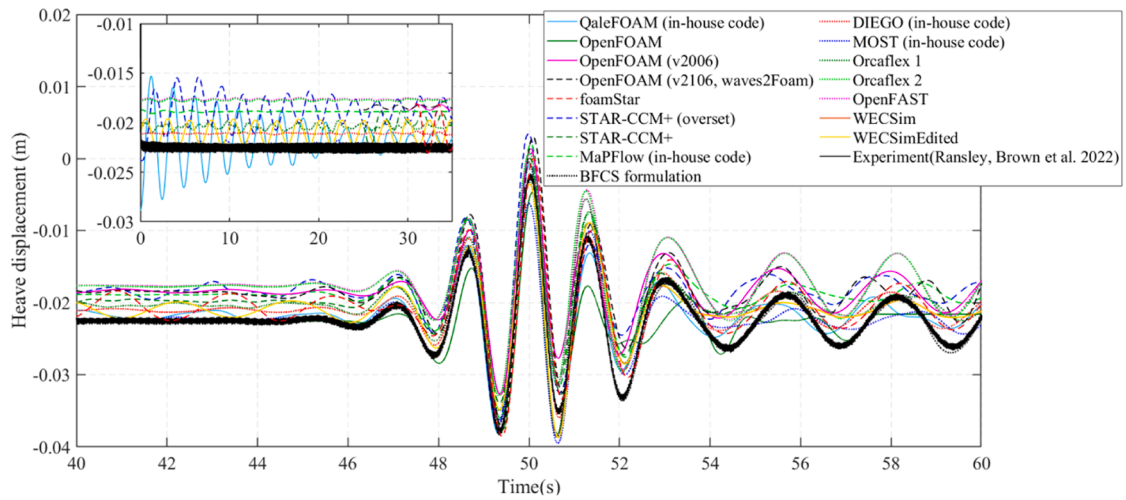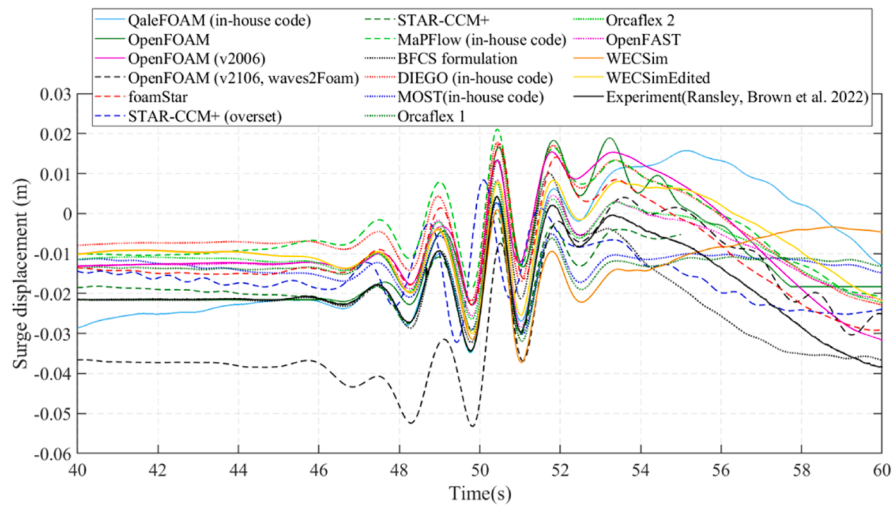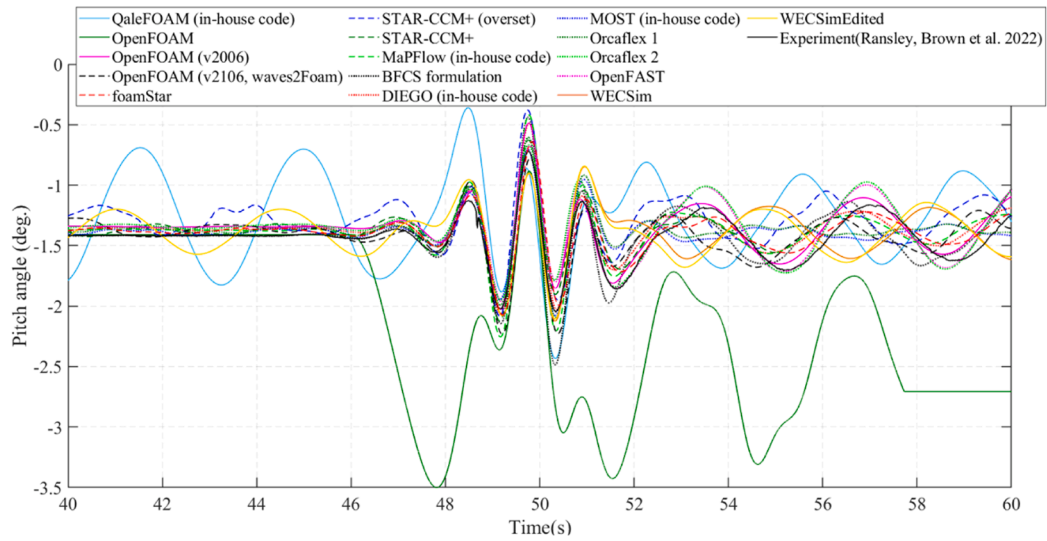
Fig. 11. Motion responses of the platform in operational focused wave case: (a) heave, (b) surge, and (c) pitch.
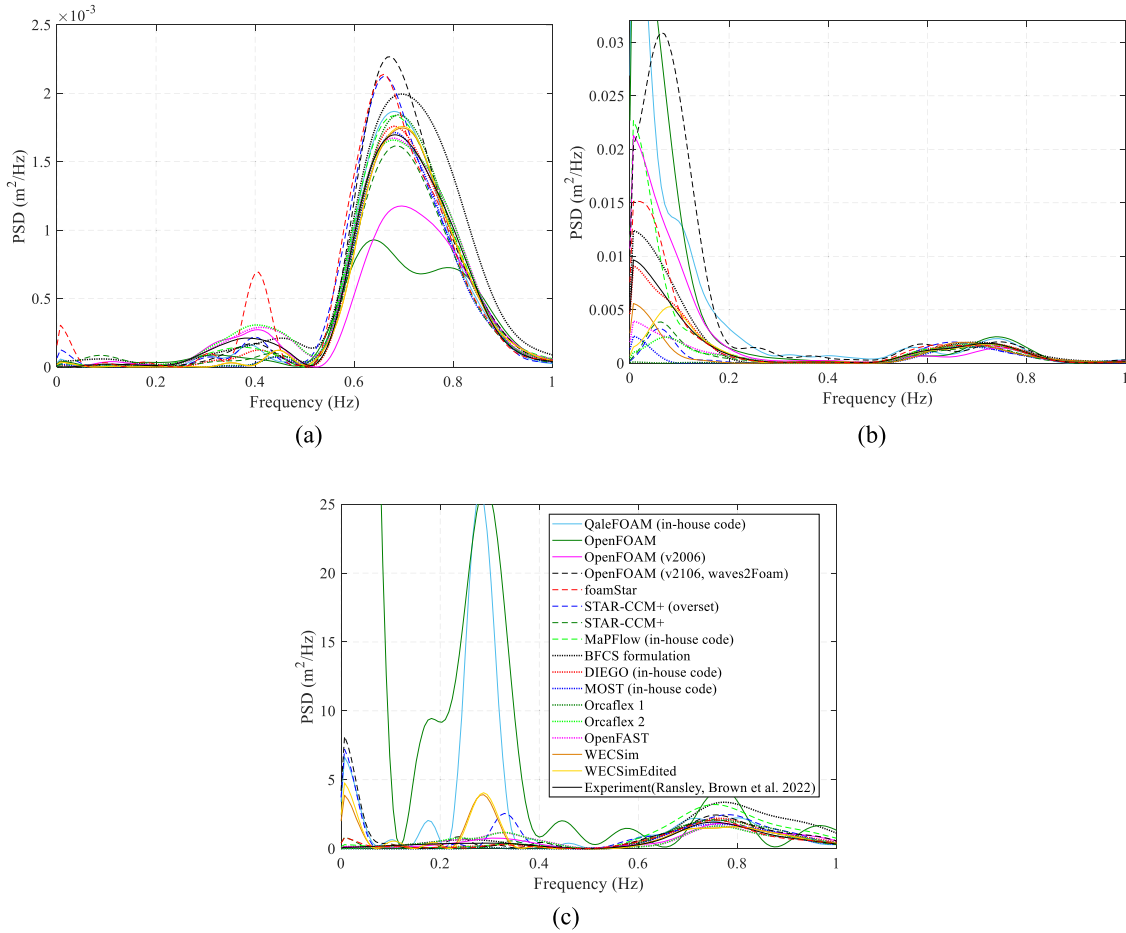
Fig. 12. PSD of the (a) heave, (b) surge, and (c) pitch motions in the operational wave case (over the range of [40.5 - 54.5] s).

the higher frequency components at the port fairlead. Note that, for better comparison of other numerical results, the result of naoe-FOAM-SJTU (in-house) at the fore fairlead is not given in Fig. 16 (c) owing to its large value.

5. Quantitative analysis of numerical models

To investigate the predictive capability of various numerical methods that participants utilized, the root mean squared error (RMSE) is calculated (Christie and Neill 2021), which can be defined as:

$$RMS\ error = \sqrt{\frac{\sum_{i=1}^{N}(\eta_n(i) - \eta_e(i))^2}{N}}$$

where N is the amount of data for analysis, and i is the ith test data; η is the time history of the wave runup or platform response in the range of focal time (in this case, [40.5 – 54.5] s) in the present study; the subscripts n and e represent the numerical and experimental value, respectively. RMSE is usually used to estimate the performance or accuracy of the predicted models, which indicates the average deviation between the predicted and the experimental values.

In Fig. 17, we present boxplots depicting the performances of various numerical approaches. Figs. 17(a) and (b) show the boxplot performances regarding the RMSE of surface elevation at different wave gauges ranging from WG3 to WG9 in the operational focused wave condition and extreme focused wave condition, respectively. We use data from WG3 to WG9 because these gauges are strategically located near the floating platform, enabling them to provide a more accurate representation of the wave patterns surrounding the platform. From

Fig. 17 (a), it can be observed that the results from the foamStar model exhibit a narrower box and the lowest median error. On the other hand, the OpenFOAM model presents the highest median error. This indicates the results are not reliable for this test case. The MOST (in-house) and Orcaflex 1 approaches, characterized by the widest box plot, seem to demonstrate the highest dispersion in the prediction of the surface elevation. Generally, the RMSE for all numerical models for operational focused wave cases is relatively low. Fig. 17 (b) reveals the comparatively inferior performance of the naoe-FOAM-SJTU (in-house) approach and the superior performance of the QaleFOAM (in-house) approach for the surface elevation in the extreme focused wave condition. In addition, less accurate results have been produced by the OpenFOAM and OpenFOAM (v2106, waves2Foam) models since their median errors are high. When viewing the RMSE at WG6 in Fig. 18, the numerical models involved here perform better for the operational focused wave case than the extreme scenario. The MOST (in-house) and Orcaflex 2 approaches have a good performance at this probe for both focused wave cases.

Fig. 19 shows the RMS errors of surge, heave, and pitch motions in the operational and extreme focused wave conditions for the different numerical approaches. It should be noted that, for the operational focused wave case, no results are shown in the figure for naoe-FOAM-SJTU (in-house), OpenFOAM (waves2Foam), and DualSPHysics models as the data are not available. From Fig. 19 (a), the QaleFOAM (in-house) approach consistently demonstrates the lowest error for the heave motion around the focal time in both operational and extreme focused wave conditions. On the other hand, models from BFCS formulation, DIEGO (in-house), MOST (in-house) and WECSim also show good performance in predicting the heave response around the
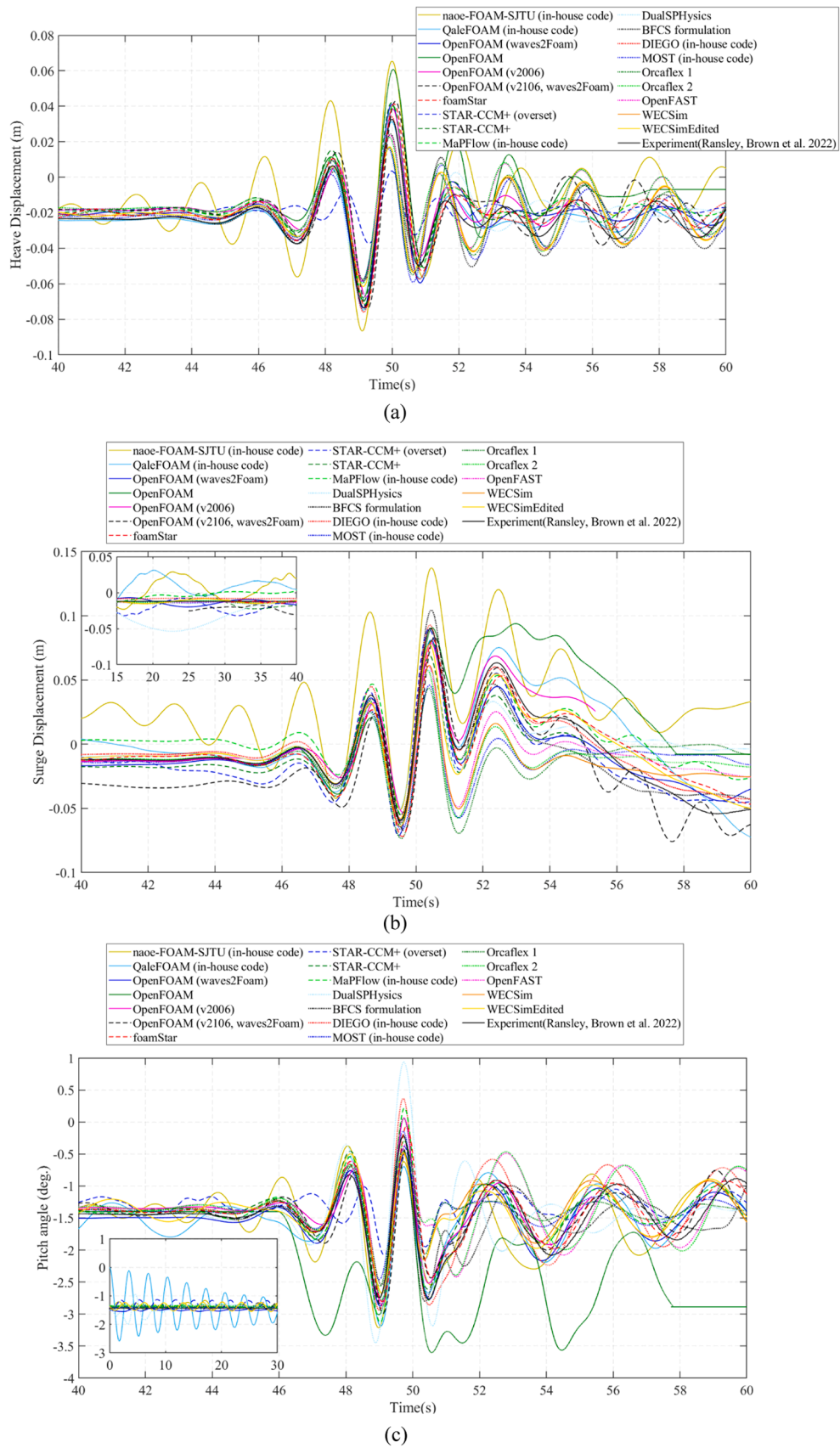
Fig. 13. Motion responses of the platform in extreme focused wave case: (a) heave, (b) surge, and (c) pitch.
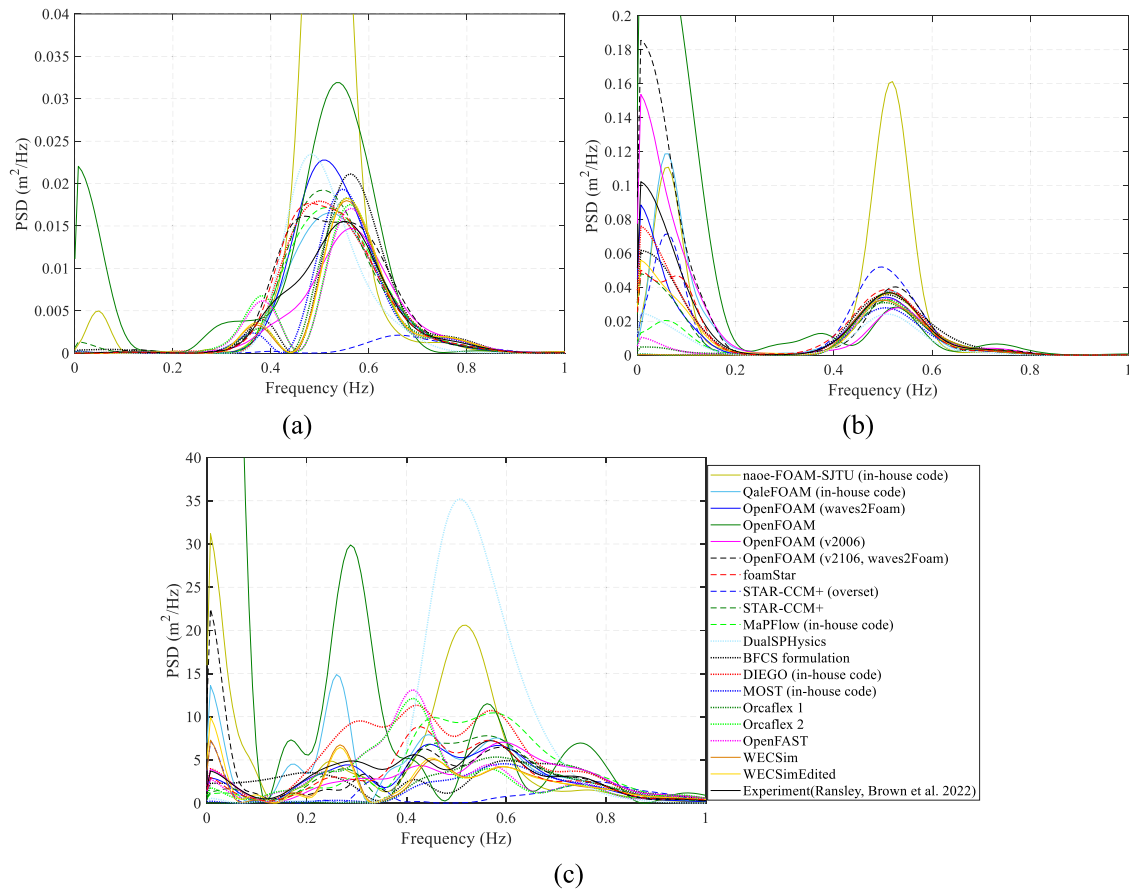
Fig. 14. PSD per frequency of the (a) heave, (b) surge, and (c) pitch motions in the extreme wave case (over the range of [40.5 - 54.5] s).
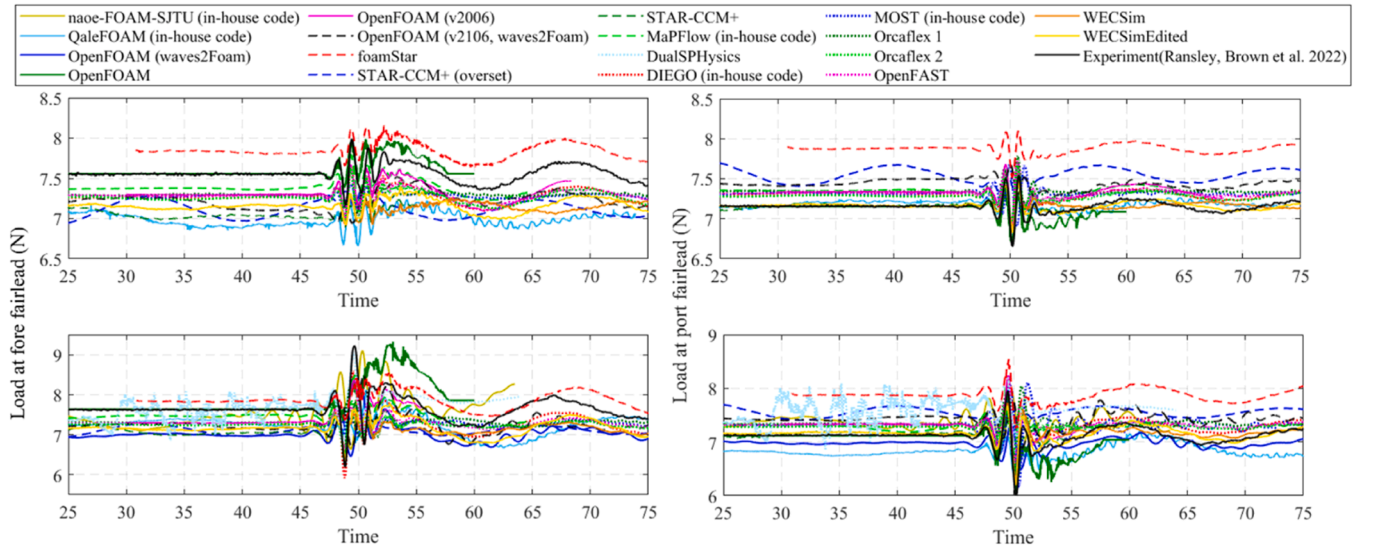

Fig. 15. Mooring loads from operational (upper) and extreme (bottom) focused wave cases at the fore fairlead (left column) and the port-aft fairlead (right column).

focal time for the operational focused wave case. This indicates that the potential flow theory-based models, if properly calibrated, can produce comparable results with those from Navier-Stokes solvers.

For the surge response as shown in Fig. 19(b), it is evident that the numerical model from STAR-CCM+ yields the lowest RMS error for the surge motion in the operational focused wave condition. While in the extreme focused wave condition, the DIEGO (in-house) approach exhibits the lowest error for the surge motion. For the pitch response

shown in Fig. 20 (c), it can be observed that the numerical models from DIEGO (in-house), MaPFlow (in-house), STAR-CCM+ and OpenFOAM (v2006) exhibit relatively smaller errors for both focused wave cases, and the lowest RMS error is achieved by the OpenFOAM (waves2Foam) model for the extreme focused wave condition. Consistent with the pitch responses displayed in Figs. 12 (c) and 14 (c), the OpenFOAM model presents the highest errors in both focused wave cases.

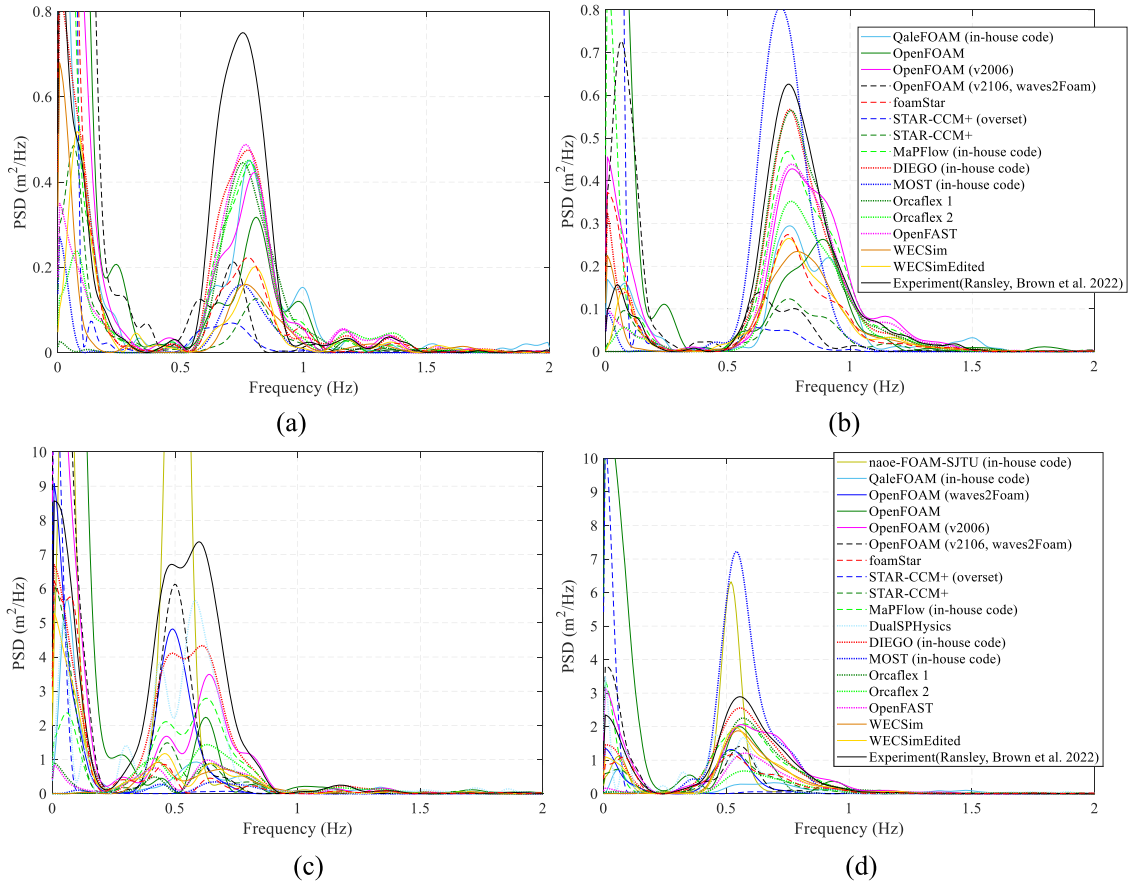From Fig. 19, it is also found that the RMS errors of most numerical

Fig. 16. PSD of mooring loads (over the range of [40.5 - 54.5]s): operational focused wave case at the fore fairlead (a) and the port fairlead (b); extreme focused wave case at the fore fairlead (c) and the port fairlead (d).
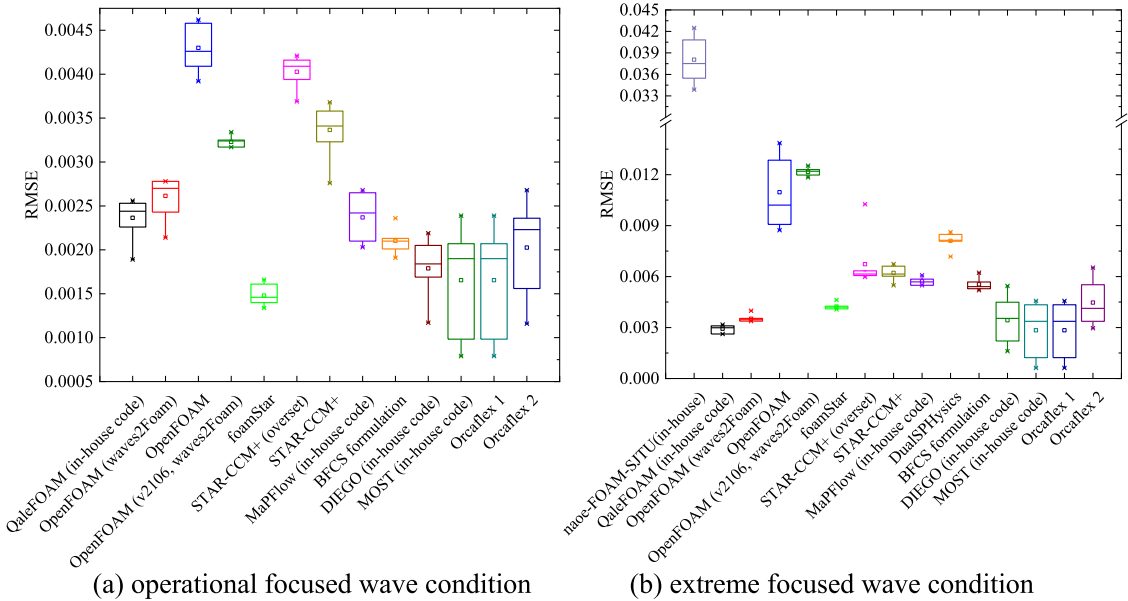

Fig. 17. The boxplots performances of distinct approaches regarding the RMSE of surface elevation.

models are lower for the operational focused wave case than the extreme condition. These models demonstrate a better performance in predicting the heave response. In addition, distinct variations in solution accuracy are observed for models using the same or similar methods (for example, STAR-CCM+ and OpenFOAM based models). Based on the overall RMS error results, the NS based solvers tend to achieve better results for the focused wave test cases especially under the extreme wave condition compared to the potential theory-based methods.
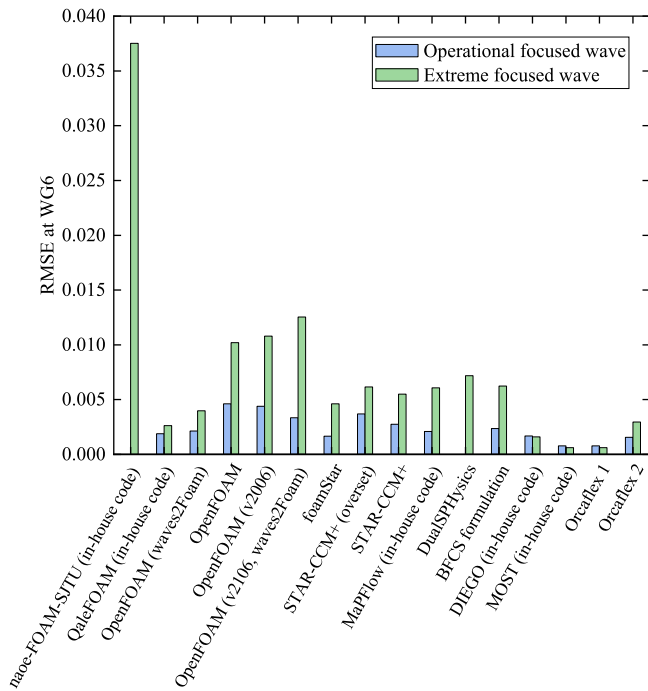
Fig. 18. RMSE of surface elevation at WG6.

6. Conclusions

This paper presents a comparative study on the hydrodynamic response of a floating offshore wind turbine model. Various numerical models ranging from linear flow models (potential flow theory and Morison equation) to the high-fidelity computational fluid dynamics method (Navier-Stokes equations) have been evaluated. Based on these numerical methods, the equilibrium positions in heave, surge, and pitch angle of the floating platform with and without moorings as well as mooring tensions in equilibrium were predicted. The heave, surge and pitch responses of the platform in the free decay tests were simulated and their natural periods and damping ratios were compared. In addition, the results for the dynamic response of the floating platform under operational and extreme focused wave conditions were analysed in both the time and frequency domains. All the numerical results were compared with the experimental data from the wave tank tests conducted in the COAST Laboratory Ocean Basin at the University of Plymouth. Main findings from the comparative study are summarised below.

1. For the static equilibrium test, as expected most numerical models predict a lower heave position for the moored FOWT model than the unmoored case. Most models underestimate the equilibrium position in heave, surge, and pitch for both cases with and without moorings except for heave without moorings compared to the physical measurements. Besides, a slightly higher tension at the port mooring line than that at the fore mooring line is predicted by most numerical models compared to the experimental tests. While the differences between the numerical results can be attributed to the differences in the numerical model setups, the differences between the numerical results and the experimental measurements could be potentially due to the underestimation of the mass values of the FOWT model.

2. In the free decay tests, the heave response of the floating platform is predicted reasonably well by all numerical models. However, the quality of surge and pitch response predictions among the numerical methods are relatively spread. Besides, most numerical models slightly overestimate the natural periods of the surge response compared to the experimental results, while slightly underpredict

the natural periods of the pitch motion. While the damping ratios predicted by most numerical methods are lower than the experimental values in all three motion directions, the potential flow models tend to under-predict the damping ratio in pitch decay by a substantial margin, indicating the inherent limitations of those models. From the comparisons, it can be shown that both high fidelity CFD models and simplified potential flow based models could perform equally 'well' or 'bad' for this test case depending on the setup of those models.

3. In the focused wave cases, the prediction of hydrodynamic response by most numerical models agrees reasonably well with the experimental results, particularly in the main crests and troughs. Compared to the heave case, the surge and pitch motions in both operational and extreme focused wave cases seem to spread more considerably among the different numerical models. In particular, significant discrepancies were present in the pitch response even between the same or similar numerical models. Highlighting the need for proper tuning and calibration (meshing, initial setup, mooring line models and time discretisation schemes and so on) of numerical models before they can be applied for modelling hydrodynamic response of FOWTs. As the wave becomes steeper, variation in results among numerical methods increases, which suggests a high demand for improved numerical methods for such issues as well.

4. Discrepancies are also found for the mooring loads among different numerical methods both at the fore and port fairleads under two focused wave cases. The higher frequency content of the mooring loads predicted from numerical mooring models tends to lag the physical measurements, particularly when the platform interacts with the severe waves. This indicates that an improved mooring model, probably with mooring line drag (Ransley, Brown et al. 2021; Eskilsson, Fernandez et al. 2023), is needed.

As a summary, in general a reasonably good agreement between numerical methods and the experimental results is identified. However, there are some variations in prediction accuracy among numerical methods. It is found that NS solvers and hybrid methods, generally, perform relatively better compared to PT and ME models. Nevertheless, some results from the NS solvers (for example, naoe-FOAM-SJTU (in-house) and OpenFOAM) present some issues in predicting the hydrodynamic response of the platform as detected from the time and frequency domains, which can be attributed to the problems in model setups, e.g., motions not starting at the equilibrium position; a poor definition of the mooring setup or a consequence of the coupling methodology used to reduce computational resources. Although the DualSPHysics model does not predict the pitch response very well with a relatively large error in the quantitative analysis, the surge and heave responses have been predicted more accurately showing the promise of the SPH method for predicting the complex wave structure interaction problems. While the PT and ME models can predict good heave responses large variations in the predicted surge and pitch motions exist and the modified WECSim model is able to predict comparable surge and pitch responses to the NS solvers and the physical measurements.

Finally, it is worth emphasising that in this comparative study, a number of contributions are from the same or a variant of the same model, e.g., OpenFOAM and Orcaflex, so the differences in the results may be attributed to the differences in individual setting up of the numerical models such as the selection of domain size, mesh type and density, and time step, etc. So, for future comparative studies, to have a fair and more meaningful comparison among different numerical models, detailed specifications on the numerical setups including initial and boundary conditions for the simulations should be provided and only spatially and temporally converged solutions be reported. However, this would not be an easy task as a large number of options/variations exist in terms of numerical models (methods), temporal and spatial discretisation schemes, meshing techniques, mooring line and turbulence models, etc. One suggested future work is to focus on the
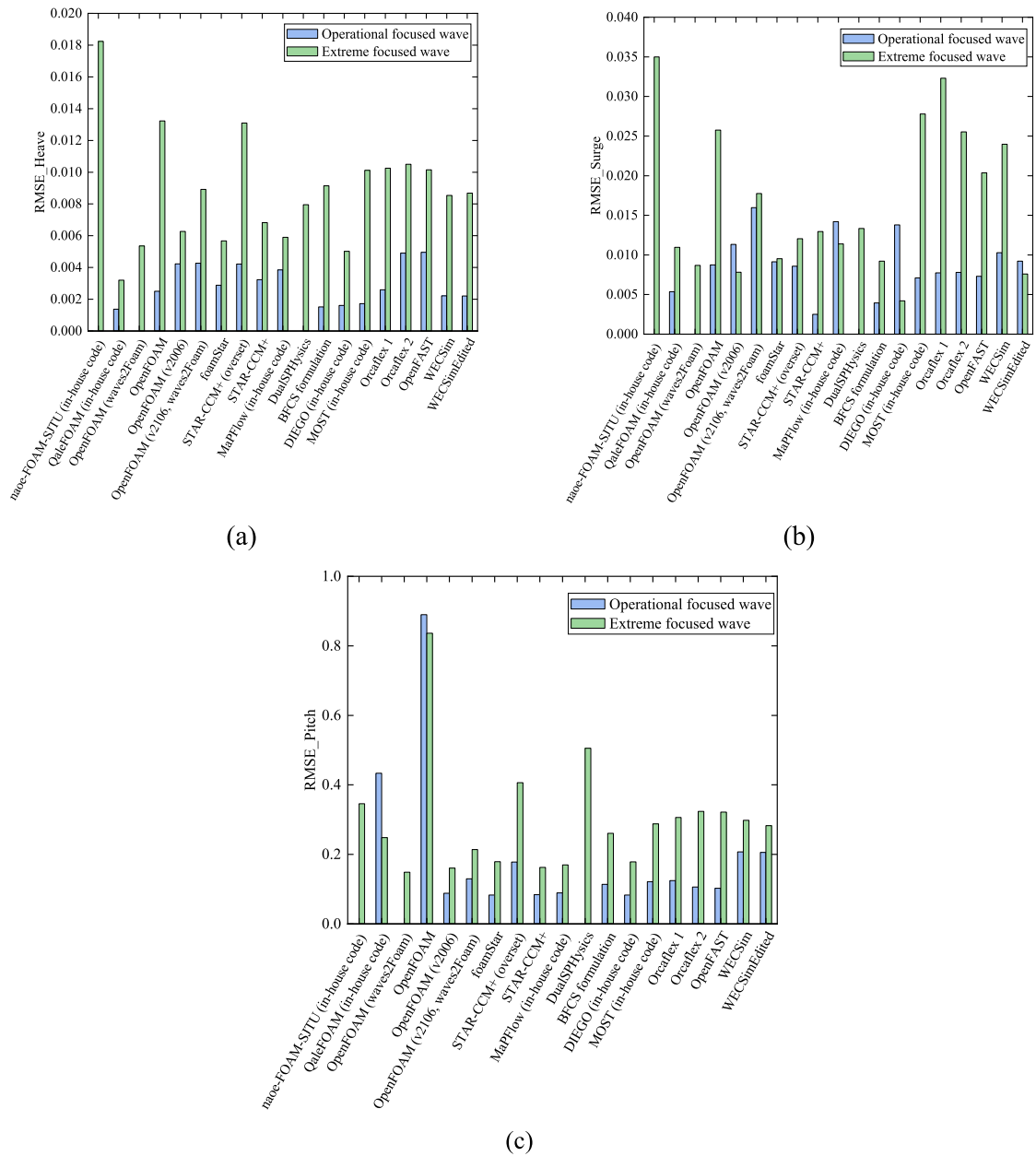
(a)

(b)

(c)

Fig. 19. RMSE of heave, surge, and pitch in operational and extreme focused waves.

comparison of the results from the same or similar flow solvers, e.g., OpenFOAM, so the underlying causes for the solution differences can be identified. On the other hand, the results compiled by this research suggest that some inaccuracies in both numerical modelling and physical modelling are inevitable. Thus, issuing guidelines that recommend acceptable discrepancies between ground truth and model predictions would be critical for the sustainability of numerical model development as past research has shown that reproducibility is not only an issue that "plagues" the numerical world, but belongs to the "nature" of things.

Declaration of generative AI and AI-assisted technologies in the writing process

Statement: During the preparation of this work the author(s) did not use any AI and AI-assisted tools.

CRediT authorship contribution statement

Shimin Yu: Writing – original draft, Visualization, Software, Investigation, Formal analysis, Data curation. **Edward Ransley:** Data curation, Writing – review & editing. **Ling Qian:** Writing – review & editing, Supervision, Resources, Project administration, Methodology, Funding acquisition, Conceptualization. **Yang Zhou:** Data curation, Writing – review & editing. **Scott Brown:** Data curation, Writing – review & editing. **Deborah Greaves:** Data curation, Writing – review & editing. **Martyn Hann:** Data curation, Writing – review & editing. **Anna Holcombe:** Data curation, Writing – review & editing. **Emma Edwards:** Data curation, Writing – review & editing. **Tom Tosdevin:** Data curation, Writing – review & editing. **Sudhir Jagdale:** Data curation, Writing – review & editing. **Qian Li:** Data curation, Writing – review & editing. **Yi Zhang:** Data curation, Writing – review & editing. **Ningbo Zhang:** Data curation, Writing – review & editing. **Shiqiang Yan:** Data curation, Writing – review & editing. **Qingwei Ma:** Data curation, Writing – review & editing. **Bonaventura Tagliafierro:** Data curation,

Writing – review & editing. **Salvatore Capasso:** Data curation, Writing – review & editing. **Iván Martínez-Estévez:** Data curation, Writing – review & editing. **Malin Göteman:** Data curation, Writing – review & editing. **Hans Bernhoff:** Data curation, Writing – review & editing. **Madjid Karimirad:** Data curation, Writing – review & editing. **José M. Domínguez:** Data curation, Writing – review & editing. **Corrado Altomare:** Data curation, Writing – review & editing. **Giacomo Viccione:** Data curation, Writing – review & editing. **Alejandro J.C. Crespo:** Data curation, Writing – review & editing. **Moncho Goméz-Gesteira:** Data curation, Writing – review & editing. **Claes Eskilsson:** Data curation, Writing – review & editing. **Gael Verao Fernandez:** Data curation, Writing – review & editing. **Jacob Andersen:** Data curation, Writing – review & editing. **Johannes Palm:** Data curation, Writing – review & editing. **Francesco Niosi:** Data curation, Writing – review & editing. **Oronzo Dell'Edera:** Data curation, Writing – review & editing. **Massimo Sirigu:** Data curation, Writing – review & editing. **Alberto Ghigo:** Data curation, Writing – review & editing. **Giovanni Bracco:** Data curation, Writing – review & editing. **Fuyin Cui:** Data curation, Writing – review & editing. **Shuling Chen:** Data curation, Writing – review & editing. **Wei Wang:** Data curation, Writing – review & editing. **Yueyue Zhuo:** Data curation, Writing – review & editing. **Yang Li:** Data curation, Writing – review & editing. **Christophe Peyrard:** Data curation, Writing – review & editing. **William Benguigui:** Data curation, Writing – review & editing. **Matthieu Barcet:** Data curation, Writing – review & editing. **Fabien Robaux:** Data curation, Writing – review & editing. **Michel Benoit:** Data curation, Writing – review & editing. **Maria Teles:** Data curation, Writing – review & editing. **Dimitris Ntouras:** Data curation, Writing – review & editing. **Dimitris Manolas:** Data curation, Writing – review & editing. **George Papadakis:** Data curation, Writing – review & editing. **Vasilis Riziotis:** Data curation, Writing – review & editing. **Zhiping Zheng:** Data curation, Writing – review & editing. **Weicheng Lei:** Data curation, Writing – review & editing. **Ruizhi Wang:** Data curation, Writing – review & editing. **Jikang Chen:** Data curation, Writing – review & editing. **Yanlin Shao:** Data curation, Writing – review & editing. **Jens Visbech:** Data curation, Writing – review & editing. **Harry B. Bingham:** Data curation, Writing – review & editing. **Allan P. Engsig-Karup:** Data curation, Writing – review & editing. **Yiming Zhou:** Data curation, Writing – review & editing. **Yefeng Cai:** Data curation, Writing – review & editing. **Haisheng Zhao:** Data curation, Writing – review & editing. **Wei Shi:** Data curation, Writing – review & editing. **Xin Li:** Data curation, Writing – review & editing. **Xinmeng Zeng:** Data curation, Writing – review & editing. **Yingjie Xue:** Data curation, Writing – review & editing. **Tiegang Zhuang:** Data curation, Writing – review & editing. **Decheng Wan:** Data curation, Writing – review & editing. **Gaspard Engel:** Data curation, Writing – review & editing. **Matthieu Tierno:** Data curation, Writing – review & editing. **Guillaume Ducrozet:** Data curation, Writing – review & editing. **Benjamin Bouscasse:** Data curation, Writing – review & editing. **Vincent Leroy:** Data curation, Writing – review & editing. **Pierre Ferrant:** Data curation, Writing – review & editing. **Gabriel Barajas:** Data curation, Writing – review & editing. **Javier L. Lara:** Data curation, Writing – review & editing.

Declaration of competing interest

The authors declare that they have no known competing financial interests or personal relationships that could have appeared to influence the work reported in this paper.

Acknowledgements

References

Allen, C., Viscelli, A., Dagher, H., Goupee, A., Gaertner, E., Abbas, N., Hall, M., Barter, G., 2020. Definition of the UMaine VolturnUS-S reference platform developed for the IEA wind 15-megawatt offshore reference wind turbine. National Renewable Energy Lab.(NREL), Golden, CO (United States). Univ. of Maine, Orono, ME (United States).

Asim, T., Islam, S.Z., Hemmati, A., Khalid, M.S.U., 2022. A review of recent advancements in offshore wind turbine technology. Energies. (Basel) 15 (2), 579.

Barajas, G., Lara, J.L., Losada, I.J., 2024. Hydrodynamic response of a floating offshore wind turbine using OpenFOAM. In: ISOPE International Ocean and Polar Engineering Conference. ISOPE.

Bergua, R., Wiley, W., Robertson, A., Jonkman, J., Brun, C., Pineau, J.P., Qian, Q., Maoshi, W., Beardsell, A., Cutler, J., 2023. OC6 Project Phase IV: validation of numerical models for novel floating offshore wind support structures. Wind Energy Science Discussions 2023, 1–36.

Bruinsma, N., Paulsen, B., Jacobsen, N., 2018. Validation and application of a fully nonlinear numerical wave tank for simulating floating offshore wind turbines. Ocean Engineering 147, 647–658.

Casiano, M. (2016). Extracting damping ratio from dynamic data and numerical solutions.

Chen, P., Chen, J., Hu, Z., 2020. Review of experimental-numerical methodologies and challenges for floating offshore wind turbines. Journal of Marine Science and Application 19, 339–361.

Cheng, P., Huang, Y., Wan, D., 2019. A numerical model for fully coupled aero-hydrodynamic analysis of floating offshore wind turbine. Ocean Engineering 173, 183–196.

Christie, D., Neill, S.P., 2021. Measuring and observing the ocean renewable energy resource. Reference Module in Earth Systems and Environmental Sciences. Elsevier, Amsterdam, The Netherlands.

Council–GWEC, G.W.E, 2023. Global wind report 2022. Global Wind Energy Council, Brussels, Belgium.

Cui, F., Chen, S., Wang, W., Zhuo, Y., Li, Y., 2023. Hydrodynamic response analysis of the Combined IEA-15-240-RWT and UMaine VolturnUS-S system to extreme loading. In: ISOPE International Ocean and Polar Engineering Conference. ISOPE.

Domínguez, J.M., et al., 2022. DualSPHysics: from fluid dynamics to multiphysics problems. Comput. Part Mech. 9 (5), 867–895. https://doi.org/10.1007/s40571-021-00404-2.

Domínguez, J., et al., 2019. SPH simulation of floating structures with moorings. Coast. Eng. 153, 103560. https://doi.org/10.1016/j.coastaleng.2019.103560.

Dunbar, A.J., Craven, B.A., Paterson, E.G, 2015. Development and validation of a tightly coupled CFD/6-DOF solver for simulating floating offshore wind turbine platforms. Ocean Engineering 110, 98–105.

Engel, G., Tierno, M., Ducrozet, G., Bouscasse, B., Leroy, V., Ferrant, P., 2023. Hydrodynamic response of a floating offshore wind turbine. In: ISOPE International Ocean and Polar Engineering Conference. ISOPE.

Eskilsson, C., Fernandez, G.V., Andersen, J., Palm, J., 2023. Hydrodynamic simulations of a FOWT platform (1st FOWT comparative study) using openfoam coupled to moodycore. In: ISOPE International Ocean and Polar Engineering Conference. ISOPE.

Eskilsson, C., Palm, J., 2022. High-fidelity modelling of moored marine structures: multi-component simulations and fluid-mooring coupling. J. Ocean. Eng. Mar. Energy 8, 513–526.

Gaertner, E., Rinker, J., Sethuraman, L., Zahle, F., Anderson, B., Barter, G., Abbas, N., Meng, F., Bortolotti, P. and Skrzypinski, W. (2020). "Definition of the IEA 15-megawatt offshore reference wind turbine".

Hall, M., et al., 2015. Validation of a lumped-mass mooring line model with DeepCwind semisubmersible model test data. Ocean Engineering 104, 590–603. https://doi.org/10.1016/j.oceaneng.2015.05.035.

Heronemus, W.E., 1972. Pollution-free energy from offshore winds. In: 8th Annual Conference and Exposition. Washington, DC. Marine Technology Society. Sep. 11-13, 1972.

Holcombe, A., Edwards, E., Tosdevin, T., Greaves, D., Hann, M., 2023. A comparative study of potential-flow-based numerical models to experimental tests of a semi-submersible floating wind turbine platform. In: ISOPE International Ocean and Polar Engineering Conference. ISOPE.

Jacobsen, N., Fuhrman, D.R., Fredsøe, J., 2012. A wave generation toolbox for the open-source CFD library: OpenFOAM®. International Journal of Numerical Methods in Fluids 70, 1073–1088.

Jagdale, S., Li, Q., Zhang, Y., Zhang, N., Yan, S., Ma, Q., 2023. A comparative numerical study of hydrodynamic response of a floating offshore wind turbine semi-submersible platform by using QaleFOAM. In: ISOPE International Ocean and Polar Engineering Conference. ISOPE.

Jonkman, J.M., Buhl, M.L., 2005. FAST User's Guide: Technical Report. National Renewable Energy Laboratory, Golden, Colorado.

Jonkman, J., Butterfield, S., Musial, W., Scott, G., 2009. Definition of a 5-MW reference wind turbine for offshore system development. National Renewable Energy Lab. (NREL), Golden, CO (United States).

Joo, J.M., 2016. Use of the logarithmic decrement to assess the damping in oscillations. Revista de Investigacion de Fisica 19, 161901551.

Larsen, T.J., Hansen, A.M., 2007. How 2 HAWC2, the user's manual. Risø National Laboratory.

Li, H., Bachynski, E.E., 2021. Experimental and numerical investigation of nonlinear diffraction wave loads on a semi-submersible wind turbine. Renew. Energy 171, 709–727.

Li, Q, Wang, JH, Yan, S, Gong, JY, Ma, QW, 2018. A zonal hybrid approach coupling FNPT with OpenFOAM for modelling wave-structure interactions with action of current. Ocean Systems Engineering 8, 381–407.

Lin, Z., Qian, L., Bai, W., 2021. A coupled overset CFD and mooring line model for floating wind turbine hydrodynamics. In: ISOPE International Ocean and Polar Engineering Conference. ISOPE.

Ma, Q., Yan, S., 2009. QALE-FEM for numerical modelling of non-linear interaction between 3D moored floating bodies and steep waves. Int. J. Numer. Methods Eng. 78 (6), 713–756.

Martínez-Estévez, I (2021). MoorDynPlus. https://github.com/imestevez/MoorDynPlus.

Menter, F., Kuntz, M., Langtry, R., 2003. Ten years of industrial experience with the SST turbulence model. In: Proc. 4th Int. Symposium on Turbulence, Heat and Mass Transfer, pp. 625–632.

Micallef, D., Rezaeiha, A., 2021. Floating offshore wind turbine aerodynamics: trends and future challenges. Renewable and Sustainable Energy Reviews 152, 111696.

Musial, W., Butterfield, S., Ram, B., 2006. Energy from offshore wind. In: Offshore technology conference. OTC.

Newmark, N, 1959. A method of computation for structural dynamics. Journal of the Engineering Mechanics Division 85 (3), 67–94.

Niosi, F., Dell'Edera, O., Sirigu, M., Ghigo, A., Bracco, G., 2023. A comparison between different numerical models and experimental tests for the study of floating offshore wind turbines. In: ISOPE International Ocean and Polar Engineering Conference. ISOPE.

Ntouras, D., Manolas, D., Papadakis, G., Riziotis, V., 2023. Hydrodynamic response of a floating offshore wind turbine using an artificial compressibility finite volume method. In: ISOPE International Ocean and Polar Engineering Conference. ISOPE.

Ntouras, D., Papadakis, G., 2020. A coupled artificial compressibility method for free surface flows. J. Mar. Sci. Eng. 8 (8), 590, 2020.

Orcina, L., 2018. OrcaFlex user manual: OrcaFlex version 10.2 c. Daltongate Ulverston Cumbria, UK.

Otter, A., Murphy, J., Pakrashi, V., Robertson, A., Desmond, C., 2022. A review of modelling techniques for floating offshore wind turbines. Wind Energy 25 (5), 831–857.

Palm, J., Eskilsson, C., 2022. Facilitating large-amplitude motions of wave energy converters in OpenFOAM by a modified mesh morphing approach. International Marine Energy Journal 5 (3), 257–264.

Palm, J., Eskilsson, C., Bergdahl, L., 2017. An hp-adaptive discontinuous Galerkin method for modelling snap loads in mooring cables. Ocean Engineering 144, 266–276.

Peyrard, C., Benguigui, W., Barcet, M., Robaux, F., Benoit, M., Teles, M., 2023. Modeling FOWT hydrodynamic behavior with comparison to basin test experiments. In: ISOPE International Ocean and Polar Engineering Conference. ISOPE.

Ransley, E.J., Brown, S.A., Greaves, D.M., Hann, M.R., 2023. Modelling the hydrodynamic response of a floating offshore wind turbine using OpenFOAM and a quasi-static mooring model. In: ISOPE International Ocean and Polar Engineering Conference. ISOPE.

Ransley, E.J., Brown, S.A., Hann, M., Greaves, D.M., Windt, C., Ringwood, J., Davidson, J., Schmitt, P, Yan, S., Wang, J.X., et al., 2021. Focused wave interactions with floating structures: A blind comparative study. Proceedings of the Institution of Civil Engineers-Engineering and Computational Mechanics 174 (1), 46–61.

Ransley, E., Brown, S., Edwards, E., Tosdevin, T., Monk, K., Reynolds, A., Greaves, D. and Hann, M. (2022). "Hydrodynamic response of a floating offshore wind turbine (1st FOWT Comparative Study Dataset)".

Ransley, E., Yan, S., Brown, S.A., Mai, T., Graham, D., Ma, Q., Musiedlak, P.H., Engsig-Karup, A.P., Eskilsson, C., Li, Q., et al., 2019. A blind comparative study of focused wave interactions with a fixed FPSO-like structure (CCP-WSI Blind Test Series 1). International Journal of Offshore and Polar Engineering 29 (02), 113–127.

Ransley, E., Yan, S., Brown, S., Hann, M., Graham, D., Windt, C., Schmitt, P., Davidson, J., Ringwood, J., Musiedlak, P.H., et al., 2020. A blind comparative study of focused wave interactions with floating structures (CCP-WSI Blind Test Series 3). International Journal of Offshore and Polar Engineering 30 (01), 1–10.

Rivera-Arreba, I., Bruinsma, N., Bachynski, E.E., Viré, A., Paulsen, B.T., Jacobsen, N.G., 2019. Modeling of a semisubmersible floating offshore wind platform in severe waves. Journal of offshore mechanics and Arctic engineering 141 (6), 061905.

Ruffini, G., et al., 2023. MESH-IN: A MESHed INlet offline coupling method for 3-D extreme hydrodynamic events in DualSPHysics. Ocean Engineering 268. https://doi.org/10.1016/j.oceaneng.2022.113400.

Rusche, H, 2002. Ph.D. thesis. Imperial College of Science, Technology & Medicine.

Salis, N., Hu, X., Luo, M., Reali, A., Manenti, S., 2024. 3D SPH analysis of focused waves interacting with a floating structure. Applied Ocean Research 144, 103885. https://doi.org/10.1016/j.apor.2024.103885.

Shao, Y., Zheng, Z., Liang, H., Chen, J., 2022. A consistent second-order hydrodynamic model in the time domain for floating structures with large horizontal motions. Computer-Aided Civil and Infrastructure Engineering 37, 894–914.

Shoemake, K, 1985. Animating rotation with quarternion curves. ACM SIGGRAPH Computer Graphics 19, 245–254.

Subbulakshmi, A., Verma, M., Keerthana, M., Sasmal, S., Harikrishna, P., Kapuria, S., 2022. Recent advances in experimental and numerical methods for dynamic analysis of floating offshore wind turbines—An integrated review. Renewable and Sustainable Energy Reviews 164, 112525.

Tagliafierro, B., Capasso, S., Martínez-Estévez, I., Göteman, M., Bernhoff, H., Karimirad, M., Domínguez, J.M., Altomare, C., Viccione, G., Crespo, A.J., 2023. Hydrodynamic validation of a semi-submersible floating platform supporting a 15MW wind turbine tower under extreme loading scenarios with DualSPHysics and MoorDyn±. In: The 33rd International Ocean and Polar Engineering Conference. Ottawa, Canada. June 19-23, 2023.

Tagliafierro, B., Karimirad, M., Altomare, C., Göteman, M., Martínez-Estévez, I., Capasso, S., Domínguez, J.M., Viccione, G., Gómez-Gesteira, M., Crespo, A.J., 2023. Numerical validations and investigation of a semi-submersible floating offshore wind turbine platform interacting with ocean waves using an SPH framework. Applied Ocean Research 141, 103757. https://doi.org/10.1016/j.apor.2023.103757.

Tan, Z., Sun, P., Liu, N., Li, Z., Lyu, H., Zhu, R., 2023. SPH simulation and experimental validation of the dynamic response of floating offshore wind turbines in waves. Renew. Energy 205, 393–409. https://doi.org/10.1016/j.renene.2023.01.081, 2023.

Tran, T.T., Kim, D.H., 2015. The coupled dynamic response computation for a semi-submersible platform of floating offshore wind turbine. Journal of wind engineering and industrial aerodynamics 147, 104–119.

Visbech, J., Bingham, H.B., Eskilsson, C., Palm, J., Engsig-Karup, A.P., 2024a. A high-order spectral element based time-domain simulation of a model-scale floating offshore wind turbine. International Journal of Offshore and Polar Engineering 34 (3), 254–262.

Wang, J, Zhao, W, Wan, D, 2019. Development of naoe-FOAM-SJTU solver based on OpenFOAM for marine hydrodynamics. Journal of Hydrodynamics 31 (1), 1–20.

Wang, L., Robertson, A., Jonkman, J.M., Yu, Y.H., 2020. Uncertainty assessment of CFD investigation of the nonlinear difference-frequency wave loads on a semisubmersible FOWT platform. Sustainability. 13 (1), 64.

Visbech, J., Engsig-Karup, A.P., Bingham, H.B., 2024b. Solving the complete pseudo-impulsive radiation and diffraction problem using a spectral element method. Comput. Methods Appl. Mech. Eng. 423, 116871.

Wendt, F., Robertson, A., Jonkman, J.M., Hayman, G., 2015. Verification of new floating capabilities in FAST v8. In: 33rd Wind Energy Symposium.

Xue, Y., Zhang, X., Zhao, W., Wan, D., 2023. Numerical study on the hydrodynamic response of a Y-shaped floating offshore wind turbine platform. In: ISOPE International Ocean and Polar Engineering Conference. ISOPE.

Zheng, Z., Lei, W., Wang, R., Chen, J., Shao, Y., 2023. Motion analysis of a moored semi-submersible floating wind turbine in focused waves by a consistent second-order hydrodynamic model. In: ISOPE International Ocean and Polar Engineering Conference. ISOPE.

Zhou, Y., Cai, Y., Zhao, H., Shi, W., Li, X., Zeng, X., 2023a. Comparative study of hydrodynamic responses of floating offshore wind turbine platform under focused wave using experiment and OpenFOAM. In: ISOPE International Ocean and Polar Engineering Conference. ISOPE.

Zhou, Y., Qian, L., Bai, W., 2023b. Sloshing dynamics of a tuned liquid multi-column damper for semi-submersible floating offshore wind turbines. Ocean Engineering 269, 113484.

Zhou, Y., Qian, L., Li, Q., 2023c. OpenFOAM modelling the equilibrium and free-decay tests of a semi-submersible FOWT model. In: ISOPE International Ocean and Polar Engineering Conference. ISOPE.